THE PENNSYLVANIA STATE UNIVERSITY
SCHREYER HONORS COLLEGE

DEPARTMENT OF CHEMICAL ENGINEERING

QUANTUM CHARACTERIZATION OF POLYMERS OF INTEREST FOR APPLICATION AS ORGANIC PHOTOVOLTAICS

GRANT ELLEDGE
SPRING 2014

A thesis
submitted in partial fulfillment
of the requirements
for a baccalaureate degree
in Chemical Engineering
with honors in Chemical Engineering

Reviewed and approved* by the following:

Enrique Gomez
Assistant Professor of Chemical Engineering
Thesis Supervisor

Michael Janik
Associate Professor of Chemical Engineering & John J. and Jean M. Brennan Clean Energy Early Career Professor in the College of Engineering
Honors Adviser

* Signatures are on file in the Schreyer Honors College.

ABSTRACT

The purpose of this research was to characterize the torsional properties of organic photovoltaics (OPVs), namely, P3HT, PBTTT, and PFOTBT. The energy as a function of the torsional angle along the bond connecting the backbone rings (e.g. thiophene rings, in the case of P3HT) was determined to quantify the likelihood of the polymer to break pi-orbital conjugation, a necessary electronic property for the target application of charge transfer along the polymer backbone.

Gaussian 09 and Gaussview were used to perform quantum chemical calculations. Due to computational restrictions, a small oligomer model for each of the polymers represented the extended polymer. An alkane functionalization representing the side chains of these polymers of at least two carbons (ethyl functionalization) was determined to be the minimum number needed; fewer carbons were clearly not representative of the model. Increasing the number of monomers above the minimum number able to represent the system demonstrated that the minimum number able to represent the system did not model the larger polymer completely accurately.

TABLE OF CONTENTS

LIST OF FIGURES

LIST OF TABLES

Chapter 1

Introduction to Organic Photovoltaics (OPVs)

Background and Need

Herein, we study the relationship between energy and torsional angle along the bond between aromatic functionalities in polymers of interest for photovoltaics (PVs), which, when using polymers as a substrate, are called organic photovoltaics (OPVs). This torsional potential is directly related to the ability of the material to conduct electrons through its conjugated backbones. The polymers *poly(3-hexylthiophene)* (P3HT), *poly[2,5-bis(3-alkylthiophen-2-yl)thieno(3,2-b)thiophene]* (PBTTT), and *poly[(9,9-di-n-octyl-2,7-fluorene)-alt-(5,5-(4',7'-di-2-thienyl)-2',1',3'-benzothiadiazole)]* (PFOTBT) were considered, as these polymers have shown promise for this application in experimental OPV research.[1,2,8-12,14,16-20]

PVs are a relatively common but minor contributor to the broader electric market. A PV takes incident electromagnetic energy, in the form of light photons, and converts it into energy. The most widely-used PV devices utilize silicon as the substrate. After the photon strikes the silicon, an electron is excited, "jumps" to another portion of the silicon, and is conducted through a circuit, producing electricity. In order for this to work, the excited electron and accompanying electron hole have to easily conduct away in the silicon to the terminals rather than simply recombining and reemitting that energy in the form of light or heat.[9,15] In order to do this, there are actually two different types of silicon in a solar cell: n-type and p-type.[2,10]

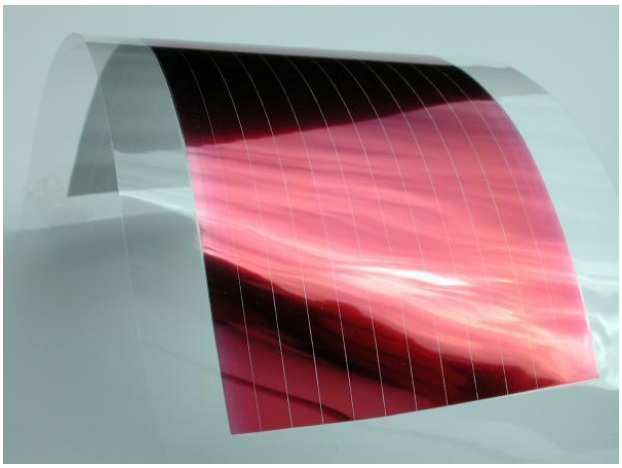

Figure 1. Flexible Photovoltaic Cell

Source: Y. Wang, University of South Florida

As concerns over energy grow globally, the world continues to lean more heavily into the investigation of potential alternative sources of energy to traditional fossil fuels. However, the classical PV is reaching limitations which further research will struggle to overcome—the price and availability of the substrate, silicon, limits the ability of PVs to be cost-competitive relative to fossil fuels and other major sources of energy, such as hydroelectric and nuclear. OPVs show promise to reduce cost: a plastic substrate would be significantly cheaper than its silicon counterpart. However, the fact that commercial PVs are still all silicon-based is indicative of the still-developing nature of the OPV.[17,18]

As it stands, there are significant problems with OPVs. The largest problem is inefficiency. The best PV developed convert on the order of 6 times as much of the incident radiation into electricity than its OPV counterpart. However, the silicon-based approach is slowly approaching an efficiency limit, the maximum amount of light which physically can be converted into electrons, due to restrictions at both the quantum and macroscopic scales. Another significant issue with OPVs is oxygen-sensitivity; most OPVs would have to be sealed from the atmosphere in order to prevent degradation of the substrate. Other issues include expense of manufacture and that the current leading method for OPV optimization is very complex.[1,2,18]

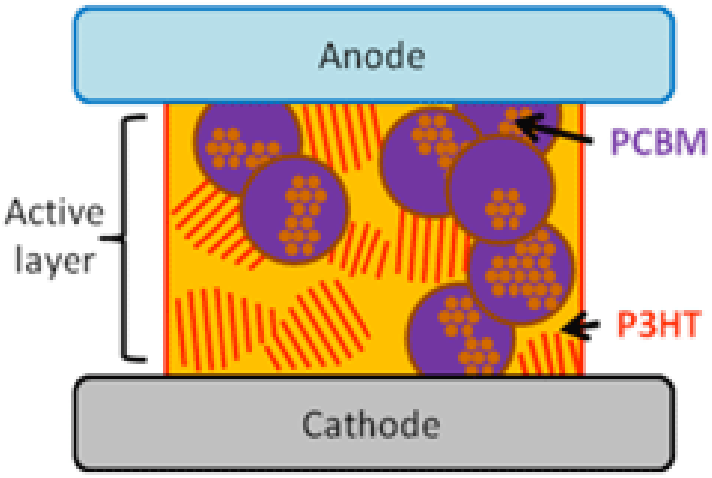

Figure 2. Schematic of OPV including polymers of interest

Source: E. Gomez, Penn State University

Expense of PVs, however, motivates the attempt to optimize the process of polymer electron conduction. This conduction is the means by which electricity is generated: a photon strikes the polymer and excites an electron, which is carried down the length of the molecule where it can "jump" to the acceptor polymer. This electron then travels down the conduction band to the cathode, does work as it passes through an external circuit, and then is reunited to the "hole" it left behind in the donor.[12,20] This sequence mirrors the way silicon-based PVs function.

PVs operate by allowing an electron to "jump" from one excited state to another between two different materials. The electron jumps from what is referred to as the "donor" to what is referred to as the "acceptor." In traditional PVs, both the donor and the acceptor are silicon; however, the donor is called n-type due to doping with a Group V element(s), often phosphorus, and the acceptor is called p-type due to doping with a Group III element(s), often boron. In the case of OPVs, the donor and acceptor are different polymers altogether, given that it is impossible to dope an organic molecule. The leading acceptors in current research are fullerenes, such as *phenyl-C61-butyric acid methyl ester* (PCBM), while the leading current donors are chains of aromatic monomers such as P3HT, PBTTT, and PFOTBT.[1,2,12,13,18]

Literature Review

The exploration of various possible acceptors and donors has received a good amount of attention in the literature. These polymers have been analyzed and characterized in various ways. The distinction between Regioregular (RR) and Regiorandom (RRa) versions on the same polymer can impact OPV performance—given that P3HT, for example, is comprised of a backbone of thiophene rings with a C_6H_{13} (or potentially longer) tail extending from one of the two carbon atoms not bonded to the adjacent ring.[16] The monomer units can be arranged with these side chains either in alternating fashion, in close proximity to each other, or with the largest possible space between. The impact of the compositional differences on OPV properties and performance is something still poorly understood.[1,18]

Another discussion in the literature revolves around some physical characterization of these polymers. Characteristics such as the absorption profile across varying wavelength are determined so as to learn more about whether the polymer will absorb photons well enough to excite a reasonable number of electrons to an excited state capable of transferring electrons to the conduction band of the acceptor. In addition, the effects of annealing of the polymer, the method of polymer deposition on the substrate, and further characteristics of these OPV models are being explored.[2,18]

Using a variety of fullerenes and possible donors such as pentacene, researchers across the globe are exploring whether compounds can successfully transfer electrons along the monomer units of a polymer, from one donor monomer to another, or from the donor to the acceptor.[13,14,20] More specifically, attempts are being made to characterize, quantify, and predictively model these factors. This work is heavily dependent on the exploration of aromatic conjugation. The idea of conjugation and its relationship to charge transfer has been significantly

explored, but little effort has been put forward to explore torsional energy potential in donor polymers.[5,7,8,11]

The key exception to the absence of work in this field is the paper titled, *Insight into how Molecular Structures of Thiophene-based Conjugated Polymers Affect Crystallization Behaviors*, authored by Liu et al.[14] Researchers from Carnegie Mellon and Central Florida calculated energetic barriers to torsional rotation for just a few models of P3HT and other compounds. Similar to my approach, the group calculated an energy-torsional angle profile, from which they determined the maximum rotation barrier. As will be seen later, the torsional profile as a whole is more relevant to the real structure of the polymer than simply the barrier, but this is a key parameter that helps us to gain an understanding of the nature of the polymer's rotation. This work included only a few model compounds, but it did indicate interest in the field on this subject matter. In order to calibrate our calculations, we ran comparable computations in order to compare results.

Fulfillment of Need

One thing that was noticed to be nearly absent in the literature by Professors Janik and Gomez was attempts to characterize a key electrical conductivity parameters of the donor polymers: the rigidity of the polymer backbone, and decided to consider the distribution of energy as a function of torsional angle as the means to determine this parameter. Due to the physical nature of the polymer matrix in an OPV, it is necessary for the electron to conduct along the backbone of the donor polymer some length before it can jump to the acceptor. Due to this fact, it is critical to understand the ability of an electron to conduct along the backbone. The singular, primary reason that aromatic functionalities are being explored for the OPV application is that they, like silicon, have the potential to be semiconductors. By nature, aromatic rings have

electrons which are delocalized in pi orbitals on either side of the ring, one of very few examples in organic chemistry of electrons with some mobility. Conjugation between adjacent aromatic rings, or the broader delocalization of these electrons, allows for the interaction among a range of delocalized states of similar energy, through which conduction may occur.

Though conduction requires long-range delocalization through aligned aromatic rings, these polymers are not rigid. Along any bond connecting the aromatic rings there exists the possibility that the conjugation will be broken as the polymer rotates along this bond. The measure of this amount of rotation is described via the torsional angle, a measure relative to a pre-determined standard that represents the amount of rotation around the center bond if viewed along the bond that is being measured. The pre-determined standard I selected was a S^1-C^1-C^2-S^2 (where the superscript represents each ring) angle of 180°. The amount that the conjugation is broken is calculated via probability functions from the energetic minima as a function of torsional angle and the barriers between these minima. From this, a parameter known as persistence length was developed, which is a numerical approximation of how many consecutive monomer units are "typically" conjugated before a break in conjugation occurs. This is one end result of the research; because it describes a physical characteristic of the polymer, it is a useful parameter for continued research in this area.

Research Methods

The large polymers of interest were simplified in order to be computationally tractable. For P3HT, which is typically comprised of hundreds of monomer units and has 6-carbon functionalization in its pure form, we first reduced the values of each of these parameters to their respective minima (two monomers and 0- carbon functionalization[14])

and then stepped up these values to five monomers and 3-carbon functionalization until we were the model size did not impact qualitative conclusions. For PBTTT, only the single monomer was considered due to its significantly larger size than the thiophene unit of P3HT. Side-chain functionalization was explored in the same manner. This is especially relevant for PBTTT given that the pure compound has 16-carbon functionalization.

In defining the ring-to-ring torsional angle, we used the S^1-C^1-C^2-S^2 angle, where superscripts 1 and 2 represent coplanar rings. At a torsional angle of 0°, the adjacent rings are coplanar with the sulfur atoms placed furthest apart (S^1-C^1-C^2-S^2 angle of 180°). The structure was then constrained at 10° intervals of the torsional angle and optimized aside from the torsional constraint. Torsional profiles show the energy at each of these 10° intervals, all of which are calculated relative to the minimum for the specific model data set.

Models were built and visualized in Materials Studio 7.0, a molecular simulation and generation software program. The coordinates of each atom's nucleus was then exported and included as a Gaussian input (.com) file. Molecular electronic structure was determined and nucleus arrangement optimized using Gaussian 09, which constrained the torsional angle in increments of 10° and calculated the energy at each optimized state. Gaussian 09 is a density-functional theory (DFT) application. DFT utilizes models of electron interactions to optimize the positions of each atom, and then calculates the energy of that state relative to the state of all of the atoms and electrons being spaced infinitely apart.[3,4]

The DFT exchanged correlation functional used was B3LYP, a common functional for organic electronic structure modeling.[4] The basis set utilized for these calculations was 6-31G**, which represents a model including *s*, *p*, and *d* orbitals. The Gaussian 09 main command input line was:

```
Opt=ModRedun b3lyp/6-31G** SCF=(MaxCycle=500)
```

The following line was placed at the bottom of the .com file to enact the torsional constraint. The *D* represents "dihedral," the following four numbers are the numbered atoms by which the torsional angle was calculated, and the final number represents the number of increments the 360° torsional profile was broken into, yielding 10° steps:

```
D 5 4 6 10 36
```

This energy data point as a function of torsional angle was visualized and explored using GaussView, energies were transferred to Microsoft Excel, and the values were converted to proper units and compared to the relative minimum point in each data set. The resultant graphs were generated from this data.

For many systems considered, the system symmetry requires the torsional profile from 180° to 360° to be a mirror image of the profile from 0° to 180°. We sampled the 180° to 360° portion to assure internal consistency. The initial structure used for atom positions for a given torsional angle is that from the optimization at the previous 10° increment, so in some cases the 0° to 180° and 180° to 360° portions identified different structural arrangements that lead to different local minima (for what should be equivalent values). In cases where these values conflicted, we adjusted input structures to find the lowest energy states.

Chapter 2

Results of Quantum Mechanical Calculations

The primary focus of this research was the analysis of energy as a function of torsional angle. All of the compounds studied have shown promise in OPV research. The primary emphasis of this research was done on the compound *poly(3-hexylthiophene)* (P3HT). Following this, torsional profiles were generated for PBTTT, *poly[2,5-bis(3-alkylthiophen-2-yl)thieno(3,2-b)thiophene]*, and PFOTBT, *poly[(9,9-di-n-octyl-2,7-fluorene)-alt-(5,5-(4',7'-di-2-thienyl)-2',1',3'-benzothiadiazole)]*. The conclusions reached from these results will be discussed, and related studies completed during undergraduate studies are reported.

Liu et al[14] Results

Liu et al, in their paper, "Insight into how molecular structures of thiophene-based conjugated polymers affect crystallization behaviors," reported torsional energy profiles for OPV-related models. In this paper, the authors Liu et al reported the average rotation barrier, or the average value of the difference between the maxima and minima in the torsional profile. I completed comparable calculations to validate accuracy of the methods used herein.

Below is a table which compares the results produced by Liu et al in comparison to our replicated models.

Table 1. Torsional Activation Barrier Results compared to Liu et al

Compound Modeled	Liu et al Barriers	Our Barriers	Percent Difference
P3HT, methyl chain	1.22 kcal/mol	1.32 kcal/mol	8.1 %
P3HT, no chain	2.70 kcal/mol	2.70 kcal/mol	0.2 %
PTzQT-14	4.95 kcal/mol	4.91 kcal/mol	0.8 %

These results satisfactorily supported the continuation of my work on compounds of interest for organic photovoltaics which had not yet been explored.

P3HT Results

High-grade P3HT is typically comprised of polymers made up of on the order of 500 thiophene ring and hydrocarbon side-chain monomer units, each of which contain 25 atoms. Due to computational limits of DFT, the complete electronic structure modeling of even one of these polymers to a reasonable degree of accuracy is impossible. As a result, simplified models of the polymer had to be explored as an estimate of the actual polymer. The main means by which the polymer was simplified were really the only two means available: the reduction of the length of the side chain and the reduction in the number of monomer units, the latter to a greater degree.

A few things quickly become apparent from analysis of data. First, increasing the number of monomer units has a measurable impact on the energy profile and barrier. Second, the extension of side chains, with the exception of when neither side chain is adjacent to the bond being torsionally constrained, has a similar measureable impact of slightly smaller order than the previous. Third, the utilization of methyl functionalization for the model of the side chain has an electronic effect which significantly alters the torsional energy profile, notably reducing the barrier to rotation. This is noteworthy because exploration of a methyl thiophene polymer is being explored for the OPV application, and because it gives us another view into the electronic delocalization and conjugation. Each of these three aspects will be explored in detail for P3HT in this section.

Thiophene Ring Models

The simplest model of a backbone bond in P3HT is a pair of bonded thiophene rings, Figure 3, with hydrogen atoms completing the valences of each carbon atom:

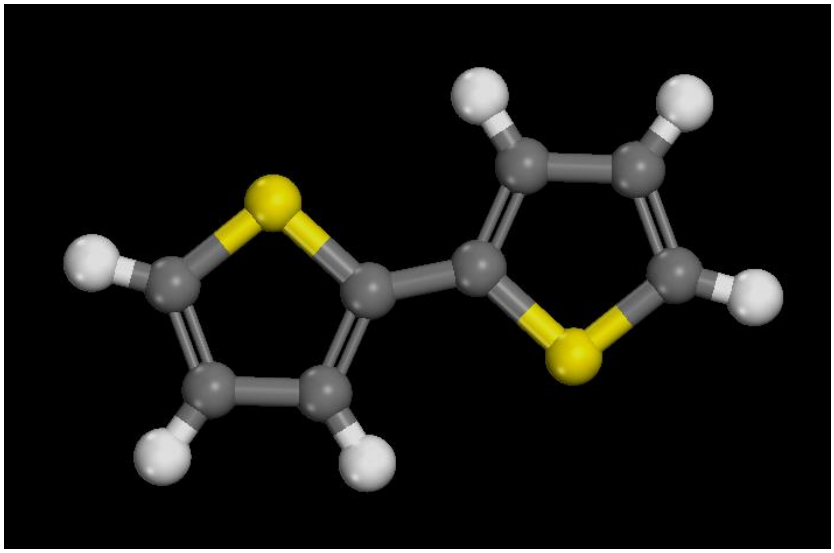

Figure 3. 2-monomer P3HT with 0-carbon side chains

This is the simplest model possible of P3HT which can be torsionally constrained. In referring to these structures, the number of carbons will be used as a reference; this model has a 0-carbon side chain. This section explores 0-carbon side chain models as an introduction. As described in the methods, the above model was constrained at each of 10° torsional intervals, and Figure 4 is the resultant energy profile as a function of torsional angle.

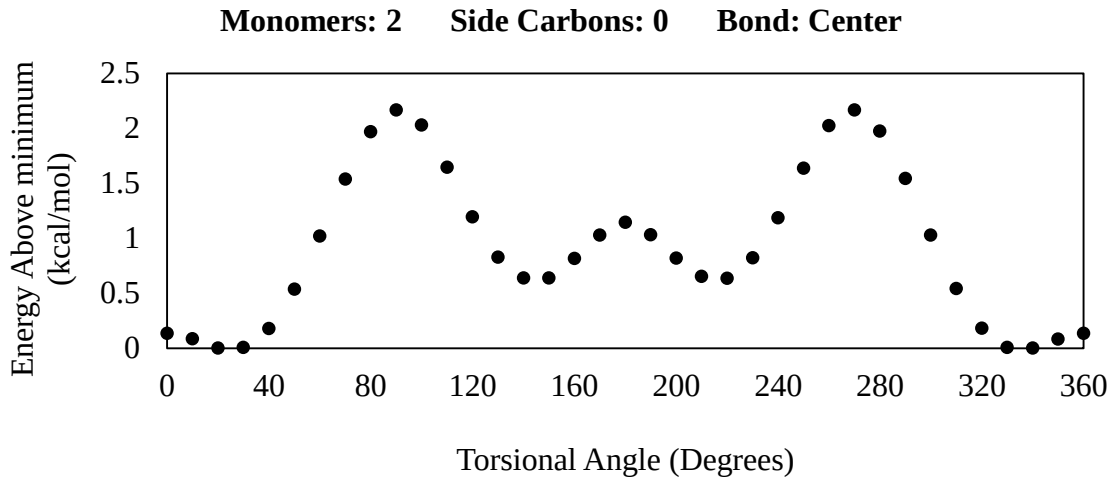

Figure 4. Torsional Energy Profile: P3HT 2-monomer with no functionalization, center bond constrained

In addition to the 2-ring model, 3-ring models were explored. In these instances, one bond was allowed to optimize freely while the other was constrained, and the optimized structure was calculated. The resultant profile is very similar:

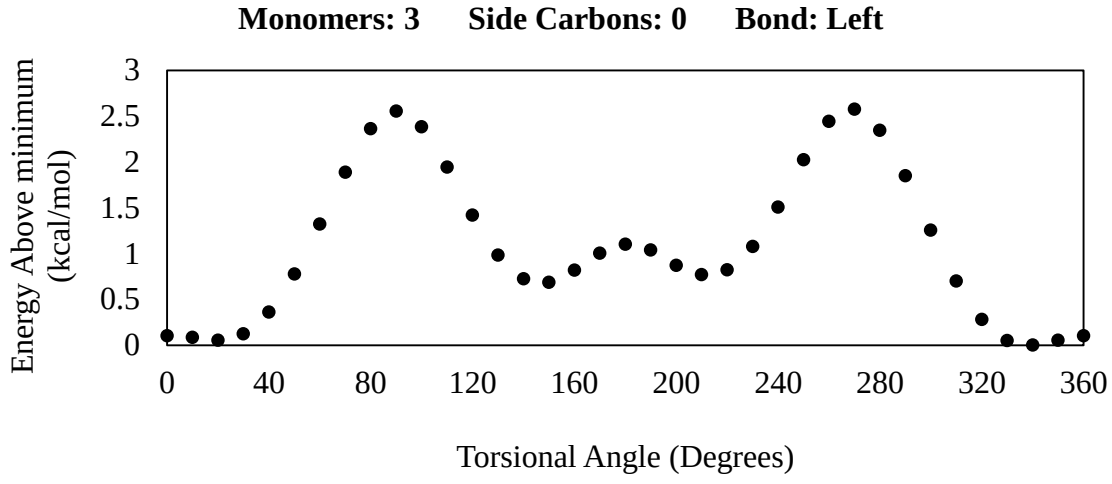

Figure 5. Torsional Energy Profile: P3HT 3-monomer with no functionalization, left bond constrained

While there is not a particularly notable difference in the construction of the profile, it is worthy of note that the maximum energy barrier is quantifiably different. We conclude that the 0-carbon side chain, 2-monomer unit model is sufficient to qualitatively converge the torsional profile.

Side Chain Modeling: 2 Monomers

We next considered the length of the carbon chains on the molecules. For both 2-ring and 3-ring P3HT, for each possible configuration and placement of the side chains, side chains comprised of 0, 1, 2, and 3 carbons were tested (hydrogen, methyl, ethyl, and propyl functionalities, respectively). We will analyze a couple sets across the range of number of carbon atoms in the side chain. All models exclude any placement of side chains on carbons adjacent to sulfur atoms, because this would then extend beyond what is considered P3HT. The vast majority of such carbon atoms would have their valences filled by an adjacent monomer unit. Before analysis of results can be discussed, however, the implementation of side chains requires the addition of nomenclature to our process.

For the 2-monomer P3HT, there are three possible positions for the pair of side chains. The first has both side chains attached to carbons adjacent to the constrained bond, and is referred to as model "A." This is the P3HT isomer model likely to yield steric hindrance upon rotation, which we will see in the results. The second has one side chain attached as above, but with the other side chain attached to the carbon further from the constrained bond, and is referred to as model "B.". This model is such that repetition of this pattern would create Regioregular P3HT. The final model has both side chains placed on the carbon further from the constrained bond, and is referred to as model "C." See Figure 6 for a depiction of these three models of two-monomer P3HT. All models below depict the 3-carbon functionality version of each type so as to clearly define the functionalization distinctions between the models.

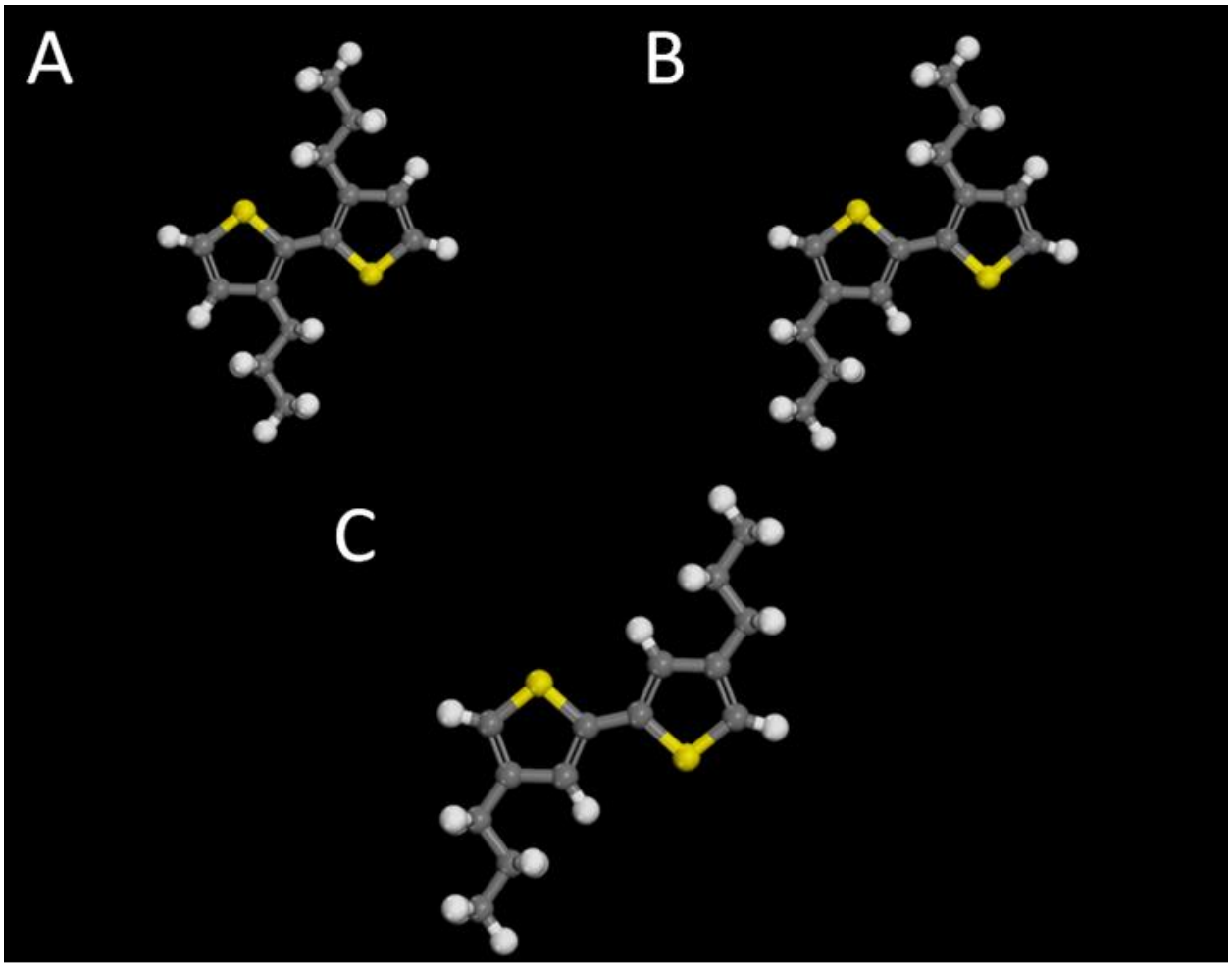

Figure 6. 2-monomer P3HT Models (all with 3-carbon side chains)

To begin, we'll investigate the model simplest to explore: 2-ring P3HT, model B. Below are the torsional profiles of each of the four different side chain lengths. The 0-carbon side chain versions of each model are identical to one another, as hydrogen functionality always exists on the non-functionalized carbon in the thiophene ring.

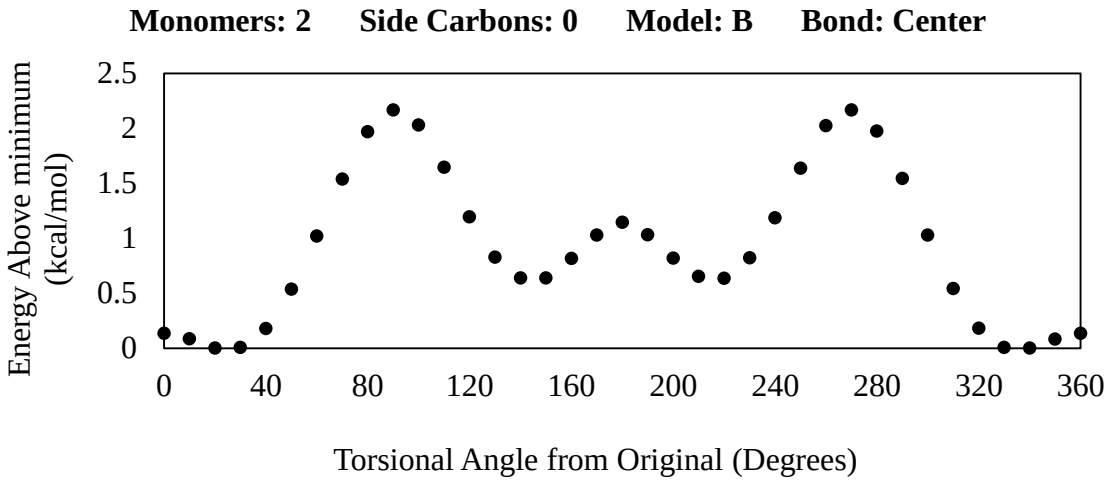
Monomers: 2 Side Carbons: 0 Model: B Bond: Center
Energy Above minimum (kcal/mol)
2.5
2
1.5
1
0.5
0
0 40 80 120 160 200 240 280 320 360
Torsional Angle from Original (Degrees)

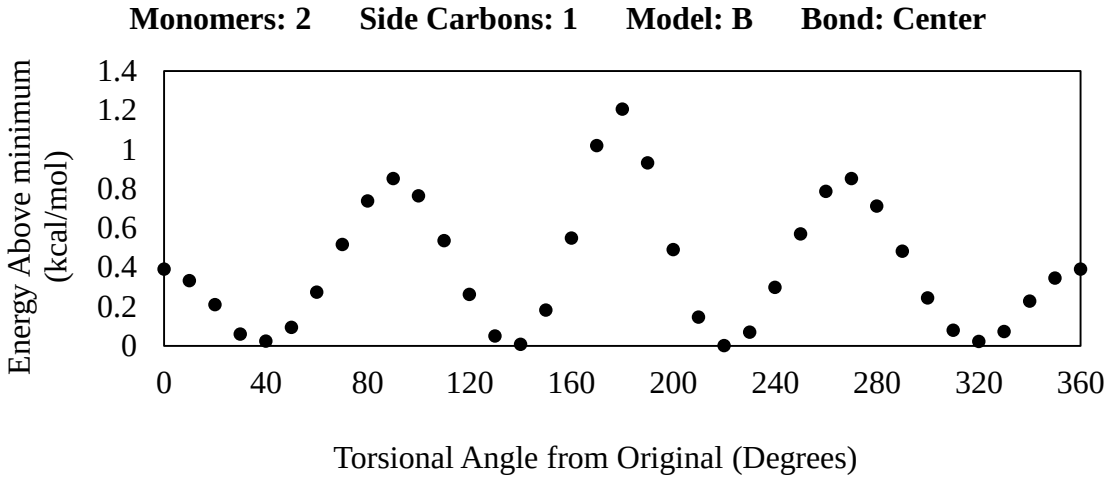
Monomers: 2 Side Carbons: 1 Model: B Bond: Center
Energy Above minimum (kcal/mol)
1.4
1.2
1
0.8
0.6
0.4
0.2
0
0 40 80 120 160 200 240 280 320 360
Torsional Angle from Original (Degrees)

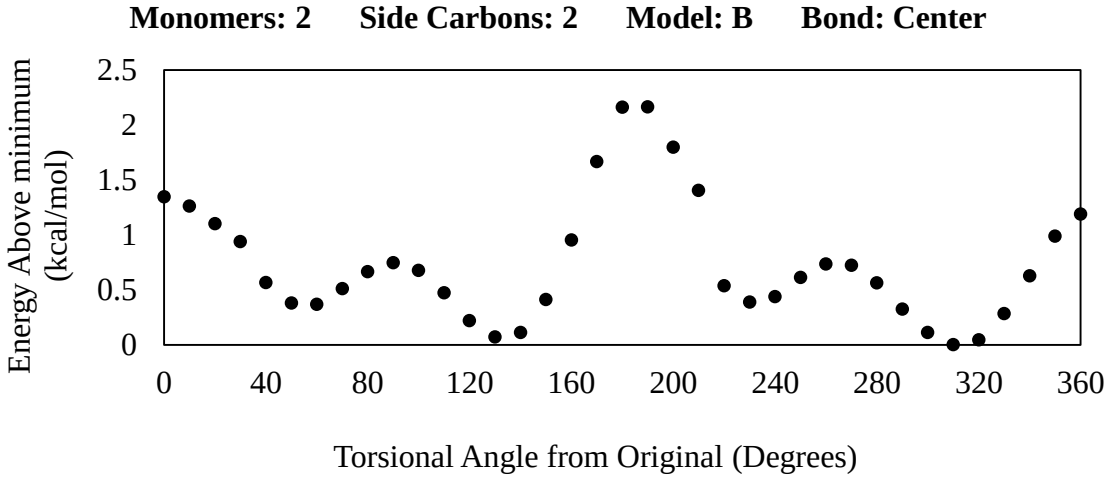
Monomers: 2 Side Carbons: 2 Model: B Bond: Center
Energy Above minimum (kcal/mol)
2.5
2
1.5
1
0.5
0
0 40 80 120 160 200 240 280 320 360
Torsional Angle from Original (Degrees)

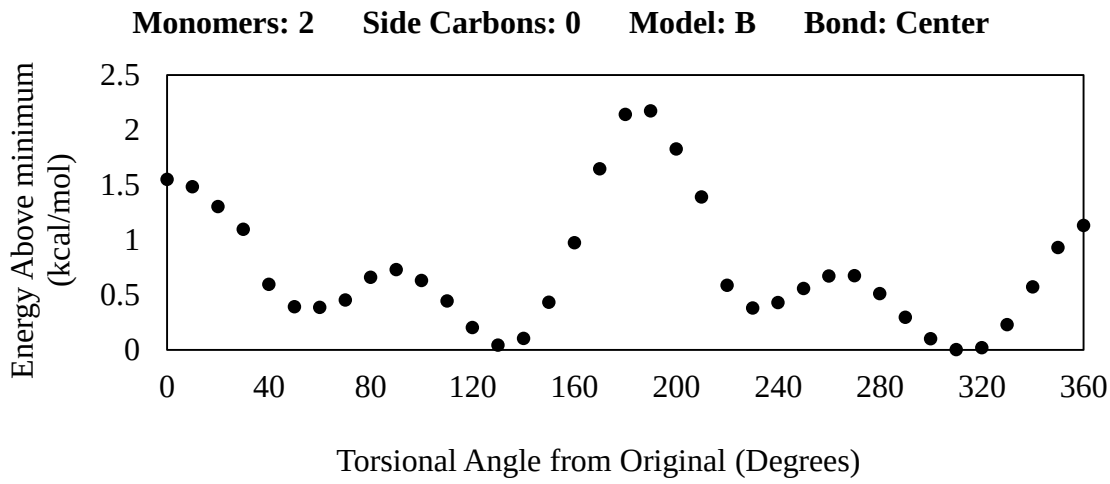

Figure 7. Torsional Energy Profile: P3HT 2-monomer Model B with each functionalization, center bond constrained

Clearly, the functionality has an impact on the torsional energy profile. It quickly becomes apparent that not only do the barriers between the minima differ in magnitude, but also the relative sizes of the peaks differ as the side chain functionality changes. The hydrogen functionality has its largest barriers to rotation when the rings are approximately perpendicular to one another, while the longer chain models have the maximum peak when the rings are coplanar and the functionalized carbons are on the same side. The methyl version of this model is perhaps the most interesting, given that it is a blend between the hydrogen side chains and longer-chain lengths and experiences a significant depression in magnitude of the relative energies of the transition stages. As discussed in the introduction, this has impacts on the fluidity of the P3HT backbone, which, in turn, impacts the conjugation of the pi orbitals of adjacent rings.

Please explore Appendix A for all of the torsional profiles of all of the models of 2-monomer P3HT. The relationships between all of the resultant calculations for 2-monomer and 3-monomer P3HT will be explored in more detail in the conclusion.

Side Chain Modeling: 3 Monomers

For 3-monomer P3HT, there are four unique combinations of placements of side chains, for a total of eight different bonds to be constrained in unique torsional models. These are in the Figure 7. Note that the "L" and "R" are abbreviations for "left" and "right", respectively, and are used in the definition of the results for each 3-monomer P3HT torsional profile. For these simulations, the indicated bond is constrained at 10° intervals and the other is allowed to rotate freely in order to find the energy minimum for each state.

The results of these optimizations were collected and grouped by a key attribute of the constrained bond—the placements of the side chains relative to this bond. The three possible combinations of relative placement match the three models of 2-monmer P3HT, and the results were grouped as such. Two of the eight combinations match each the type of 2-monomer Models A and C, and the remaining four match 2-monomer Model B. This is a helpful method to determine the accuracy of each type of model.

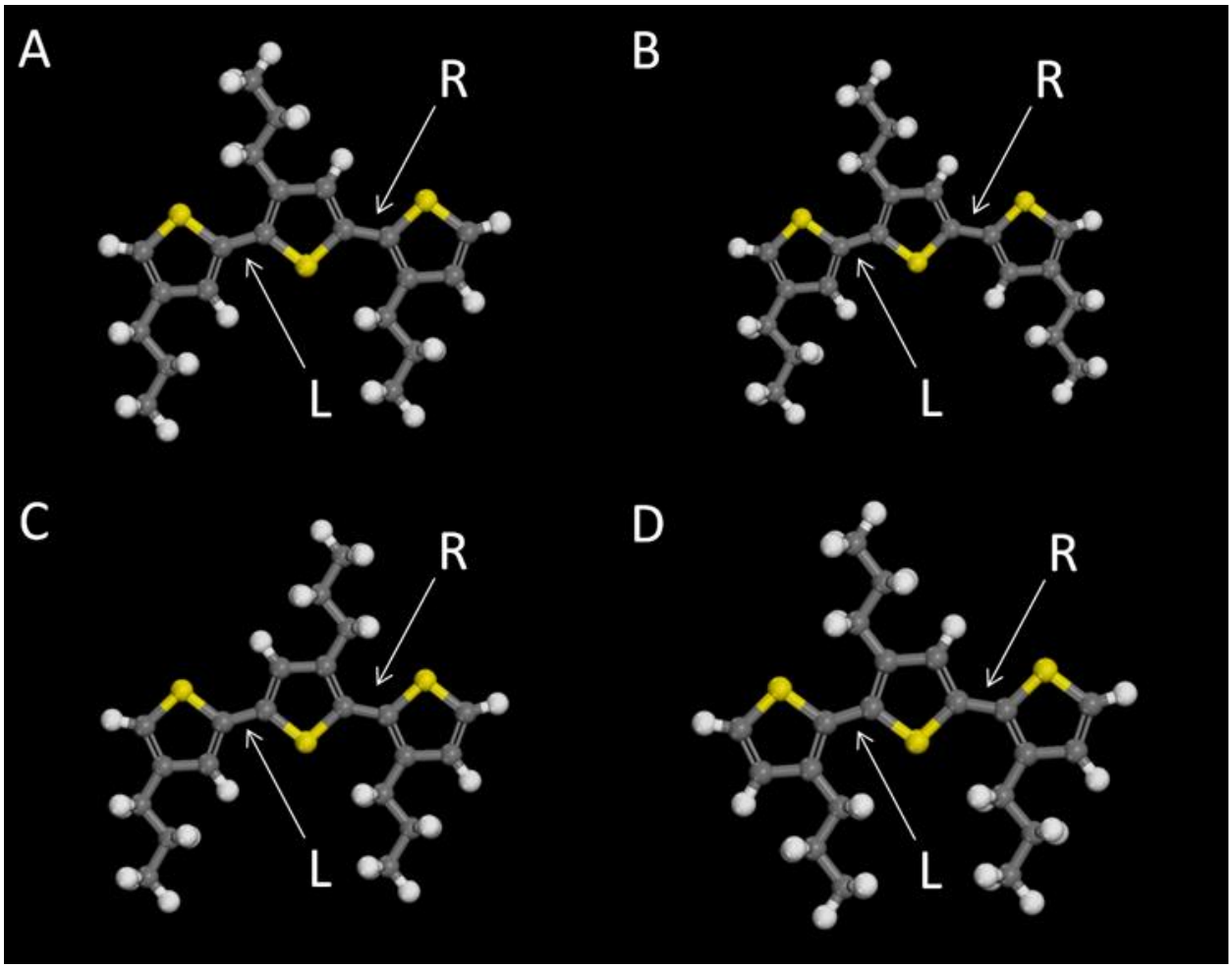

Figure 8. 3-monomer P3HT Models (all with 3-carbon side chains)

Please explore Appendix A for all eight sets of torsional profiles and the conclusion for a more thorough analysis and the results of this modeling. The results are generally comparable to those of the 2-monomer model, but with a slight increase in the magnitude of the rotational barriers, as a general rule. A further analysis of the significance of this modeling will also be explored in the conclusions and discussion section.

Long-chain Results

We considered the impact of the number of thiophene rings for methyl-functionalized P3HT. The results tend to differ as the number of rings away from the bond being constrained changes. Below is a plot demonstrating the effect of increasing the number of rings in the model. For the larger molecules, the bond nearest the end was constrained in each of these cases in order to establish comparability.

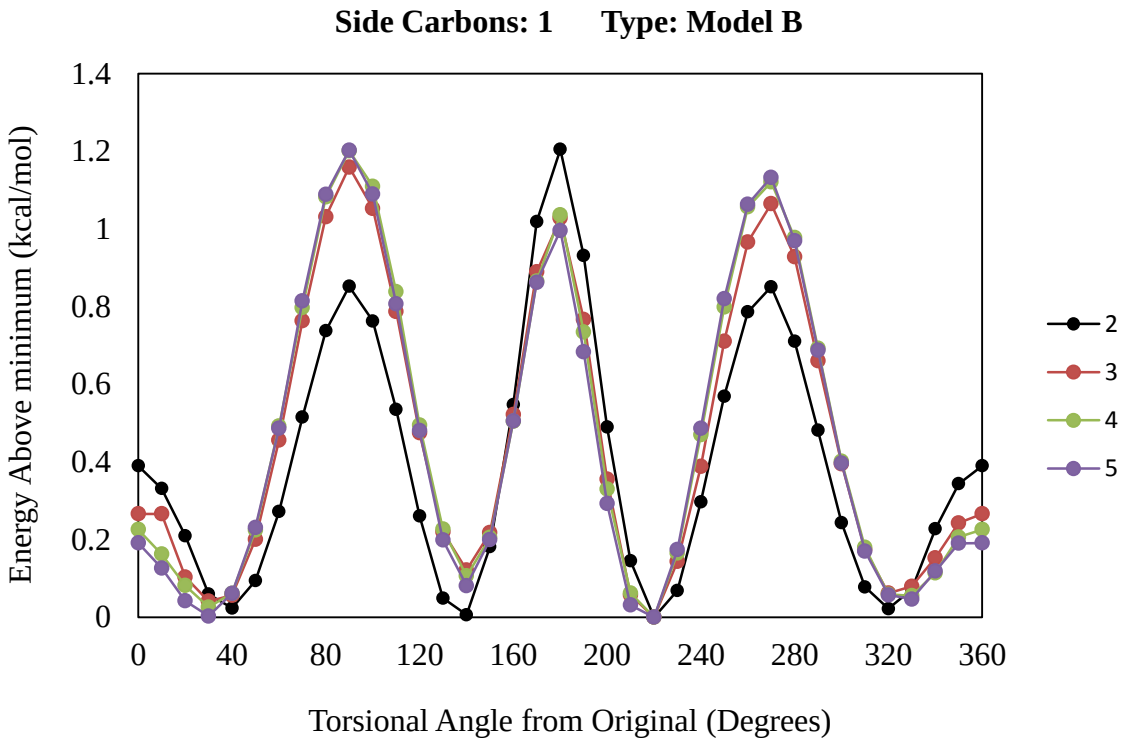

Figure 9. Long-chain models of Regioregular P3HT with methyl functionailty

It is most clear that a 2-monomer model simply does not quite represent the true structure, both in terms of the magnitude of the peaks as well as the relative sizes of each, which is potentially an even more relevant parameter.

PBTTT Results

PBTTT is a significantly larger molecule in its monomer form than thiophene. Due to this, the models tested were only one monomer, and the placement of the side chains was varied. PBTTT is either functionalized on the two single thiophene rings or on the two fused thiophene rings, as can be seen in the models below:

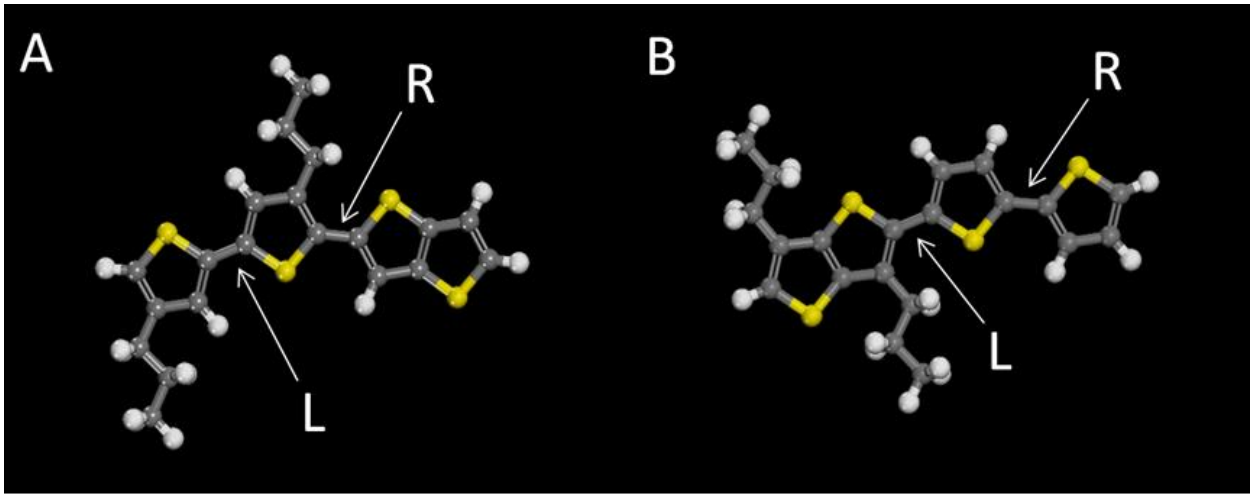

Figure 10. PBTTT Models (all with 3-carbon side chains)

The profiles for PBTTT, in comparison to P3HT, exhibit somewhat similar characteristics, although with fewer features. The set of models included in the set represented by A above, tested on the left bond, are depicted in the following graphs:

Side Carbons: 0 Model: A Bond: Left

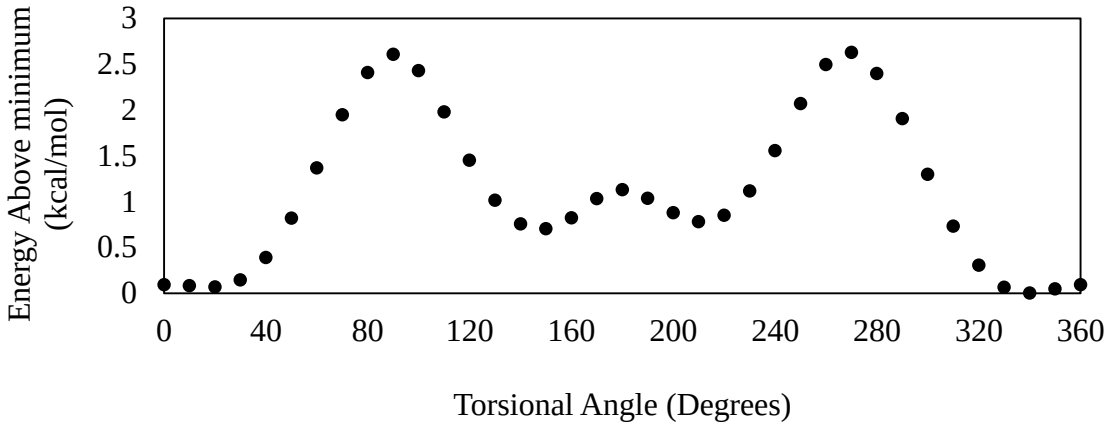

Side Carbons: 1 Model: A Bond: Left

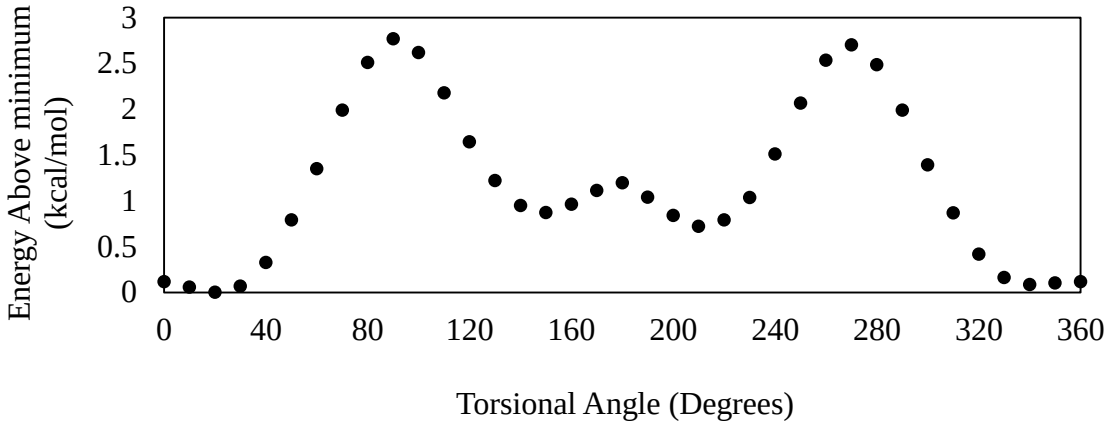

Side Carbons: 2 Model: A Bond: Left

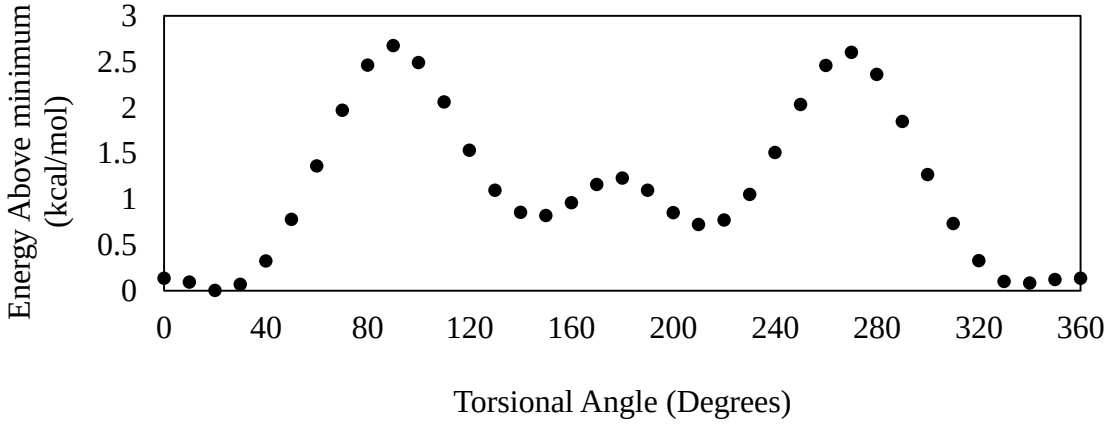

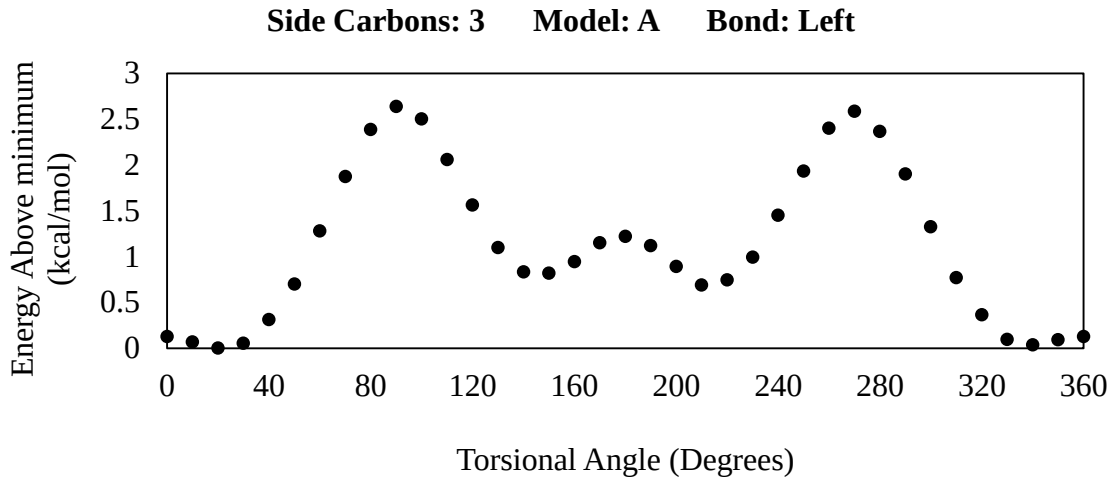

Figure 11. Torsional Energy Profile: PBTTT, Model A, Left Bond, each functionalization

The discussion will include a comparison between PBTTT and P3HT of similar type and placement of side chains, as applicable. Unfortunately, most of these results involve the constraining of only one side chain near enough to the bond to be relevant, and so instead of seeing the results of two equally-sized functionalities interacting, we see the relationship between whatever functionality and what is equivalent to hydrogen functionality. Given that the sizes of the side chains in the P3HT models were increased simultaneously, there exists no direct comparison of these results. Similarly to the results for P3HT, please explore Appendix B for a complete set of resultant profiles of P3HT modeling.

Chapter 3

Discussion and Conclusions

There are a few major questions to be answered by the data produced. The first is the relationship between the number of monomers in the model and its effectiveness. It is somewhat readily apparent that a simple, 2-monomer model is ineffective in modeling what is likely to be approaching the true system, namely the large models which were generated. The convergence of torsional profiles as more monomer units are added suggest 3 thiophene rings are sufficient to capture a reasonable torsional profile.

The future direction of this research is to expand this work into the larger potential models, utilizing increasing accessibility to computing power. At any phase, these results can and have been implemented into the calculation of persistence length, an important feature which is desired to be characterized in the determination of the properties of polymers of interest for photovoltaics. In addition to these, there are multiple ways research could progress beyond the scope of this work. One of the main reasons for the significant size of this research is that it is simply impossible to model the true polymer. Because computational cost scales with the cube of the number of atoms modeled using density-functional theory, in order to complete within a reasonable time scale, models significantly reduced the polymer scale. This includes, but is not limited to, a reduction in the number of monomers and a reduction in the length of side chains modeled. Computationally, more accurate and detailed modeling could be employed. In addition, further attempts to demonstrate that these models are truly approaching the actual system would be beneficial. Finally, a clear direction in which to carry this work is to work with the characterization of the overall system, potentially even a model of the physical OPV system.

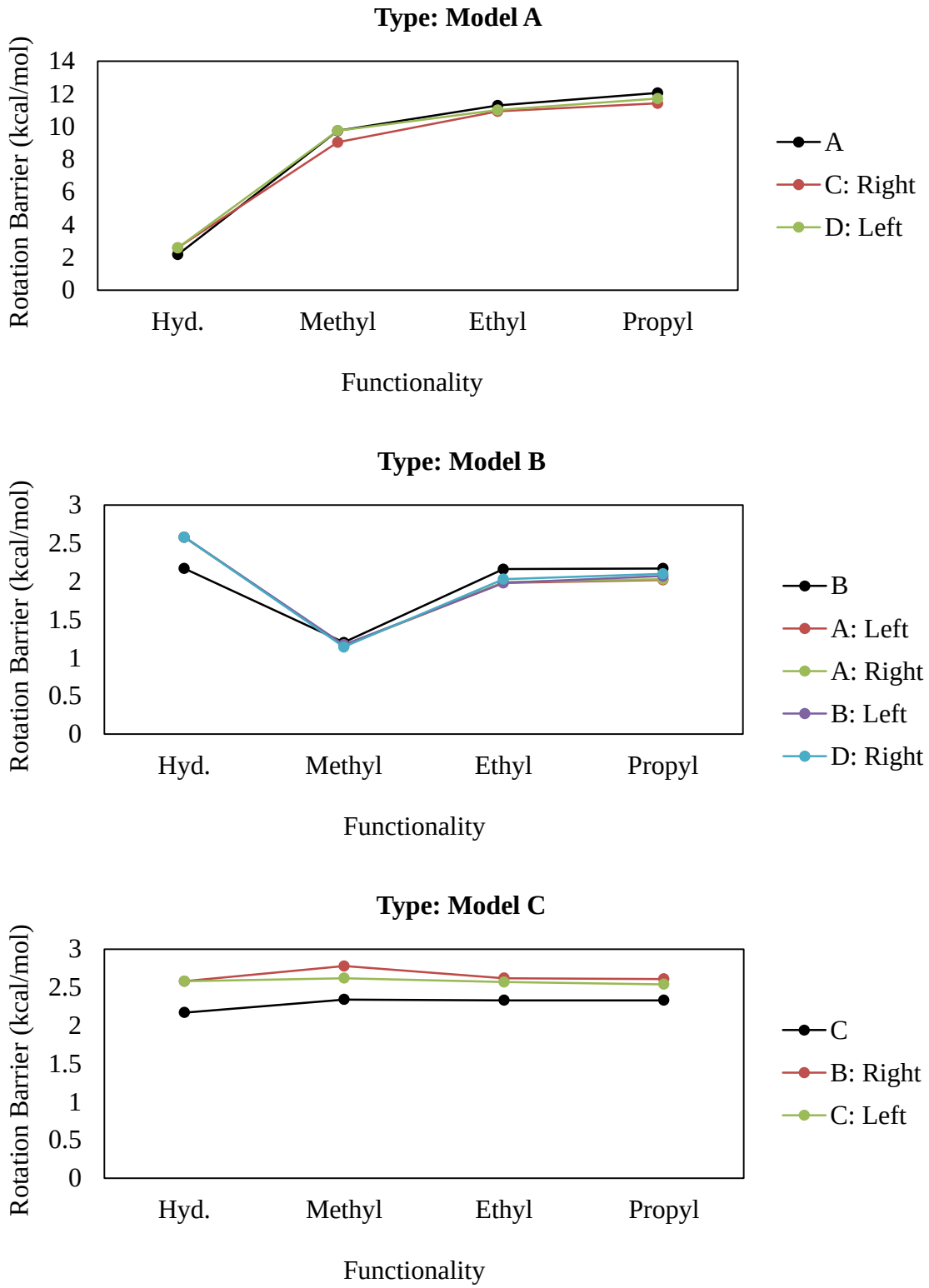

Figure 12. P3HT Rotation Barriers as a Function of Functionality, grouped according to relative placement of functionality

Discussion of Effect of Modeling Size

Another major question resolved is regarding the necessity of effective side chain modeling. Clearly, there are significant issues in utilizing hydrogen functionality as a model, and the methyl functionality also yields torsional profiles inconsistent with longer chains, particularly in the type of Regioregular P3HT. On the following page are graphs of similar side chain placement as a function of the model type and functionality. Models which are unspecified as to left or right are 2-monomer models of P3HT, while specified models are 3-monomer. From this, we can see the approach to accurate modeling occurring to varying degrees, with the relative effectiveness of the model increasing with the distance separating the two side chains relative to the bond being constrained.

Similarly, PBTTT demonstrates a quantifiable difference between the two models. The barriers for PBTTT are generally comparable to those of P3HT, especially in the cases in which the bond being torsionally constrained has alkane functionality on either side of the bond; the left bond of Model A for PBTTT is most similar to the P3HT models, and the results are comparable. The similarities in these profiles can be seen in Appendix A.

Discussion of Persistence Length

A key motivation behind this research was to determine the "stiffness" of the polymer backbone of the donor polymers. This is useful to quantify because the rings in the backbone of the polymer need to be conjugated in order for the electron to conduct and produce electricity. Persistence length is a quantity designed to describe the typical number of consecutive monomer units which are conjugated. The distribution of energy as a function of torsional angle is utilized in the calculation of the persistence length.

Specifically, the persistence length of a typical portion of the polymer is employed in the expression

$$\langle t_i \cdot t_{i+j} \rangle = \exp\left(-\frac{j}{N_p}\right)$$

where t_i is the i^{th} unit vector along the backbone (unit vectors alternate between bonds connecting two thiophene rings and an imaginary line connecting two such bonds), j is the number of units away from i, and N_p is the persistence length. This equation indicates that there is exponential decay in the straightness of the polymer backbone, typically. Wenlin Zhang, a graduate student in Penn State's Department of Chemical Engineering, has continued the research on this topic. For P3HT, he has reported a typical persistence length of approximately eight to ten monomer units. This indicates that, typically, eight or ten consecutive thiophene rings are conjugated (therefore conductive) before a break in this conjugation.

Appendix A

Selection of Relevant Torsional Profiles: P3HT

This appendix is the collection of energy as a function of torsional angle compiled for all possible arrangements of two-monomer and three-monomer P3HT, which includes, in addition to the number of rings, the placement of equivalently-sized hydrogen, methyl, ethyl, and propyl functional groups which would be considered simplified models of regioregular (RR) or regiorandom (RRa) P3HT. Each of the following graphs is labeled with the number of monomers in the model, the number of carbons in the functionalization, the model letter for the number of monomers in the model, and the bond which was constrained in the optimization.

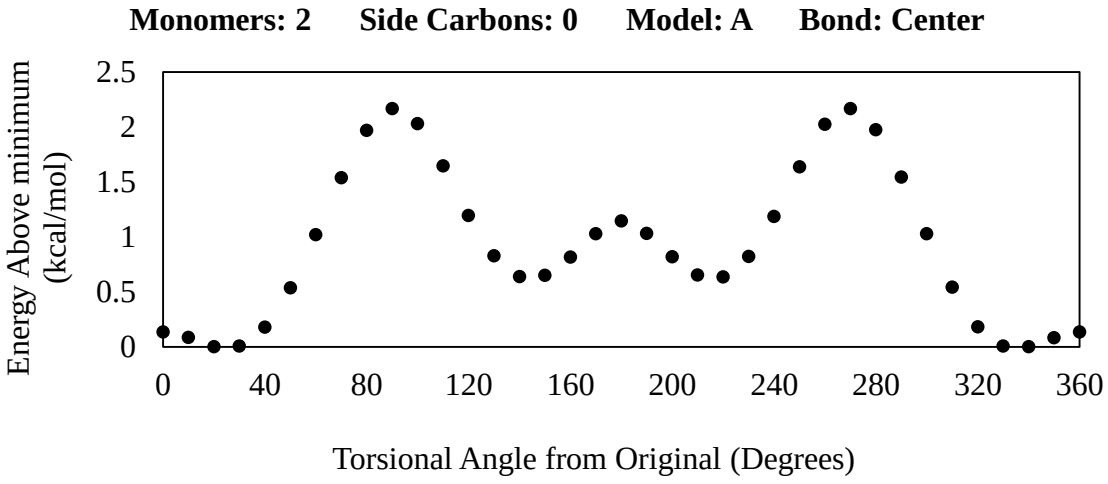

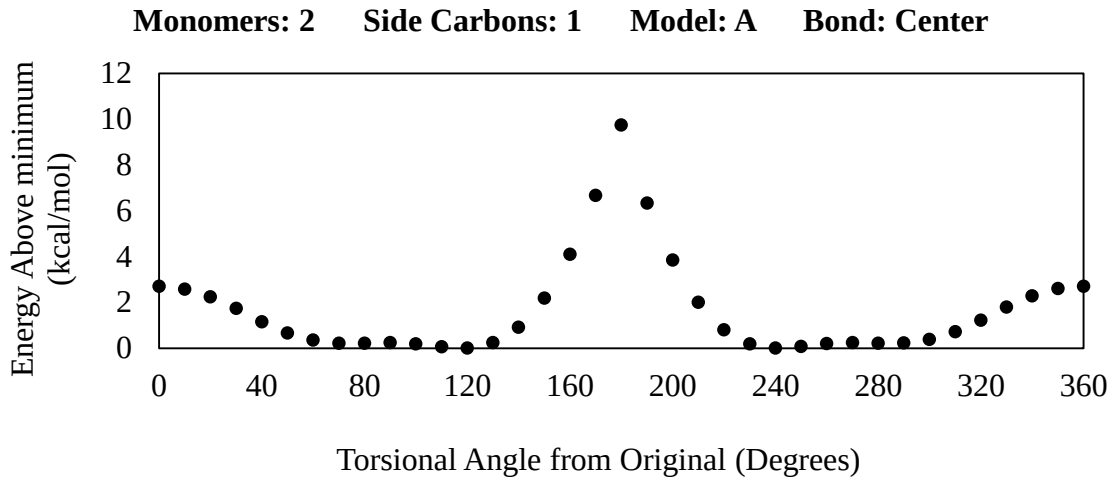
Monomers: 2 Side Carbons: 1 Model: A Bond: Center
Energy Above minimum (kcal/mol)
0
2
4
6
8
10
12
0
40
80
120
160
200
240
280
320
360
Torsional Angle from Original (Degrees)

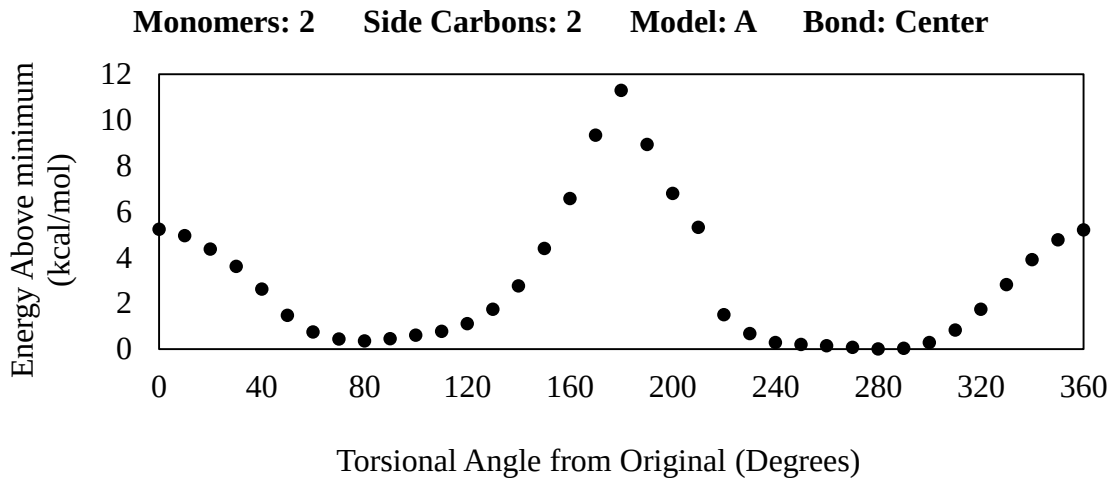
Monomers: 2 Side Carbons: 2 Model: A Bond: Center
Energy Above minimum (kcal/mol)
0
2
4
6
8
10
12
0
40
80
120
160
200
240
280
320
360
Torsional Angle from Original (Degrees)

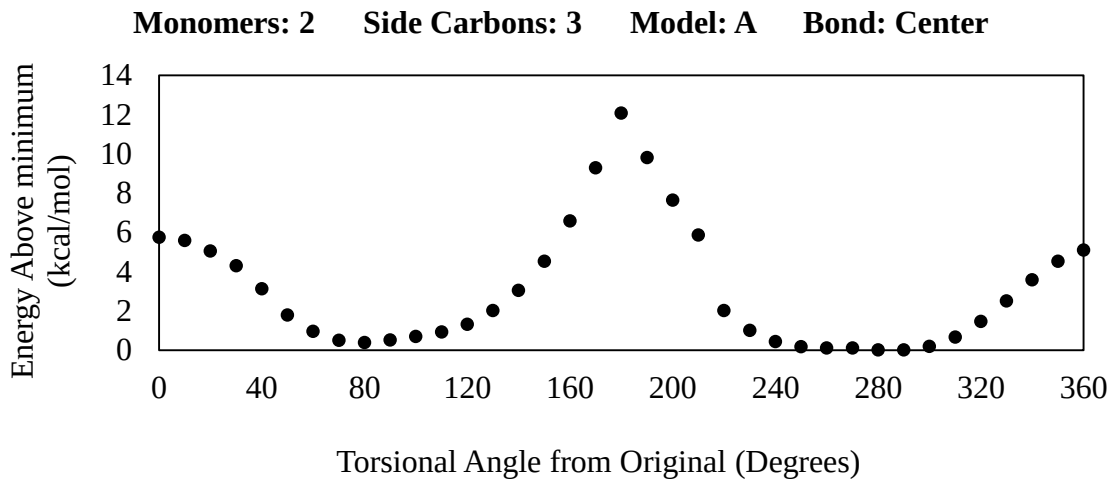
Monomers: 2 Side Carbons: 3 Model: A Bond: Center
Energy Above minimum (kcal/mol)
0
2
4
6
8
10
12
14
0
40
80
120
160
200
240
280
320
360
Torsional Angle from Original (Degrees)

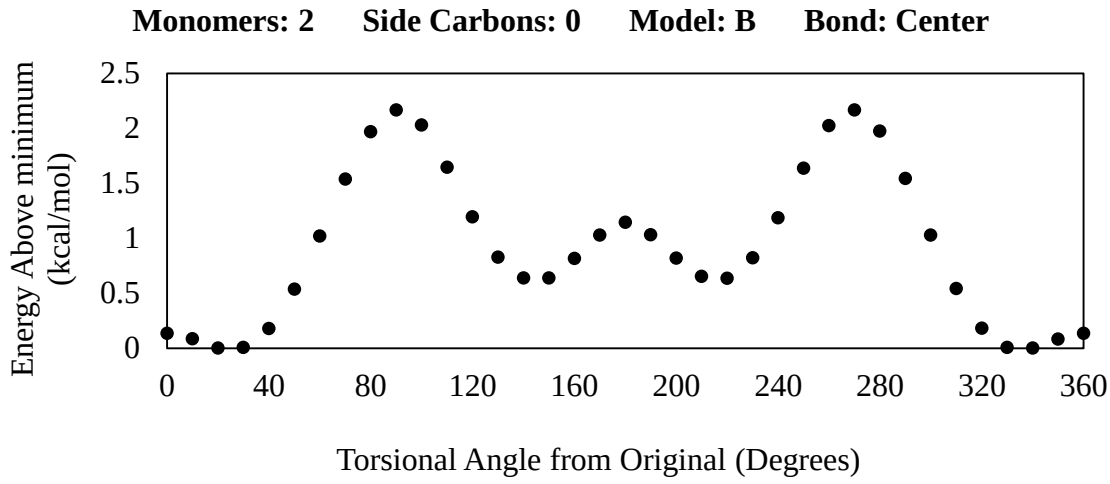
Monomers: 2 Side Carbons: 0 Model: B Bond: Center
Energy Above minimum (kcal/mol)
2.5
2
1.5
1
0.5
0
0 40 80 120 160 200 240 280 320 360
Torsional Angle from Original (Degrees)

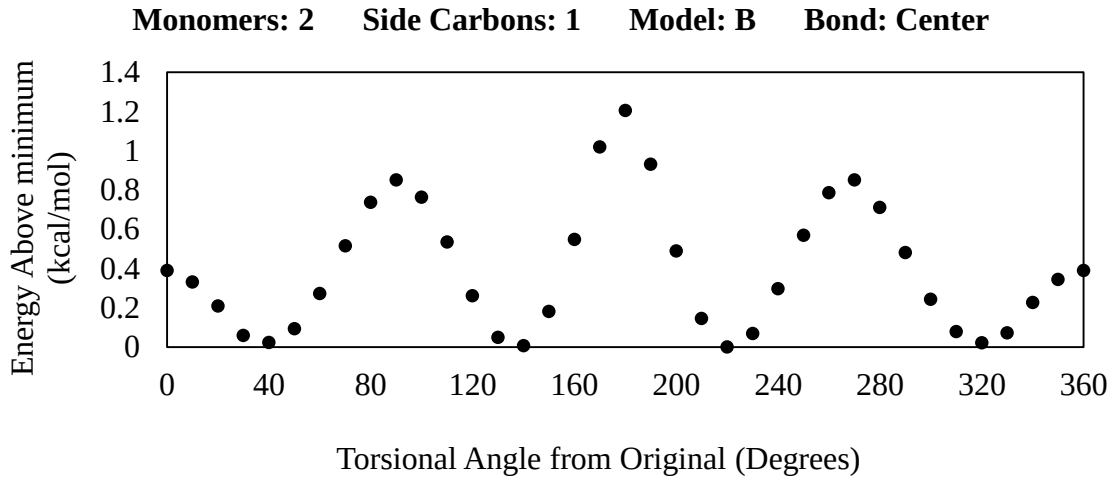
Monomers: 2 Side Carbons: 1 Model: B Bond: Center
Energy Above minimum (kcal/mol)
1.4
1.2
1
0.8
0.6
0.4
0.2
0
0 40 80 120 160 200 240 280 320 360
Torsional Angle from Original (Degrees)

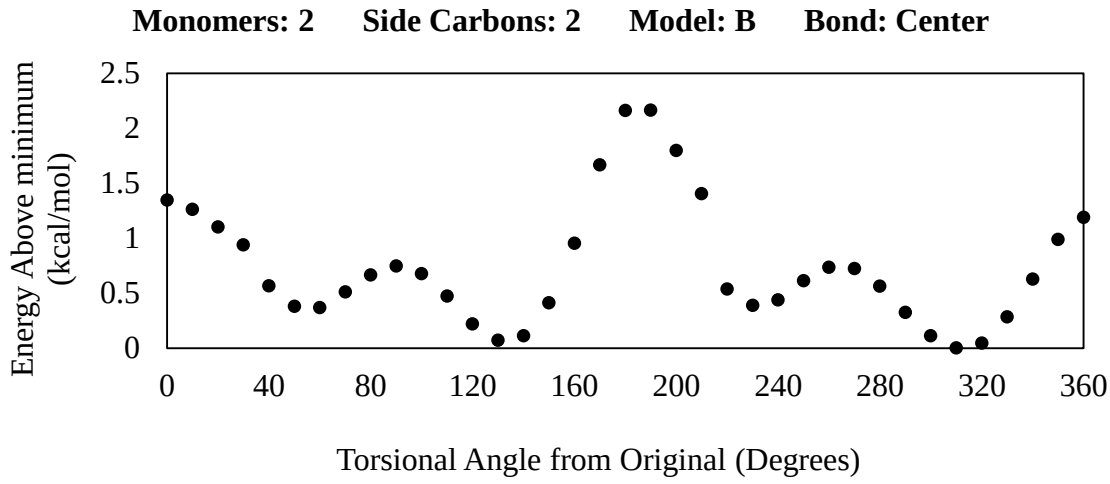
Monomers: 2 Side Carbons: 2 Model: B Bond: Center
Energy Above minimum (kcal/mol)
2.5
2
1.5
1
0.5
0
0 40 80 120 160 200 240 280 320 360
Torsional Angle from Original (Degrees)

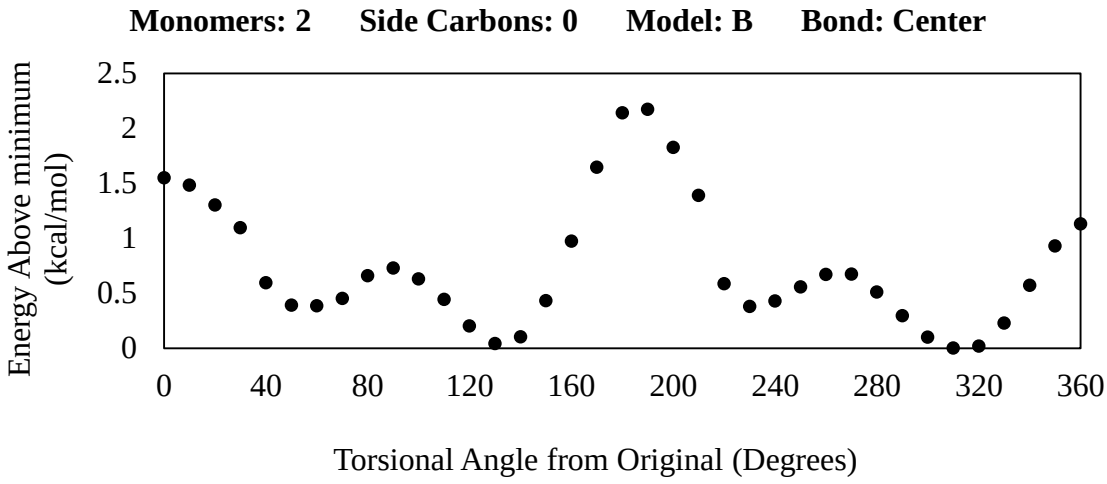
Monomers: 2 Side Carbons: 0 Model: B Bond: Center
Energy Above minimum (kcal/mol)
2.5
2
1.5
1
0.5
0
0 40 80 120 160 200 240 280 320 360
Torsional Angle from Original (Degrees)

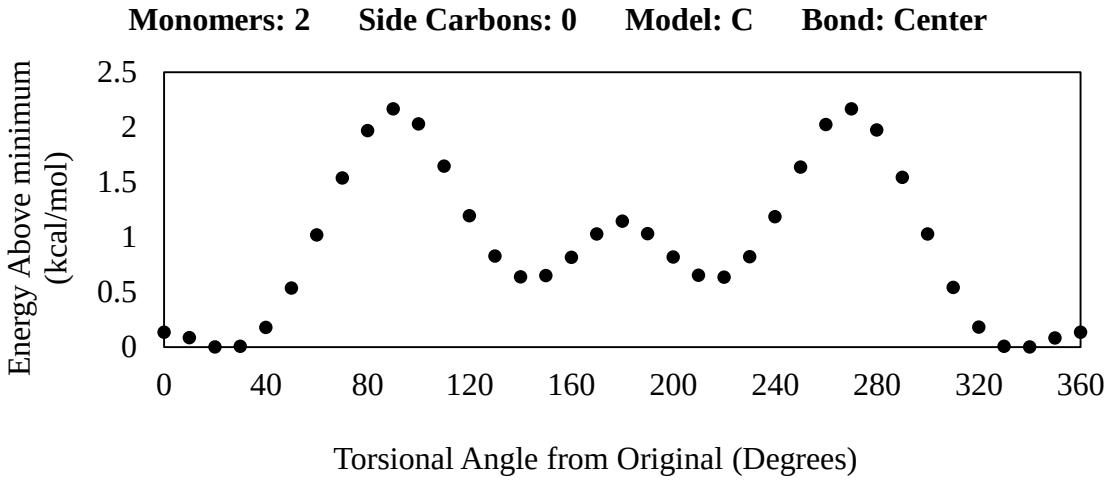
Monomers: 2 Side Carbons: 0 Model: C Bond: Center
Energy Above minimum (kcal/mol)
2.5
2
1.5
1
0.5
0
0 40 80 120 160 200 240 280 320 360
Torsional Angle from Original (Degrees)

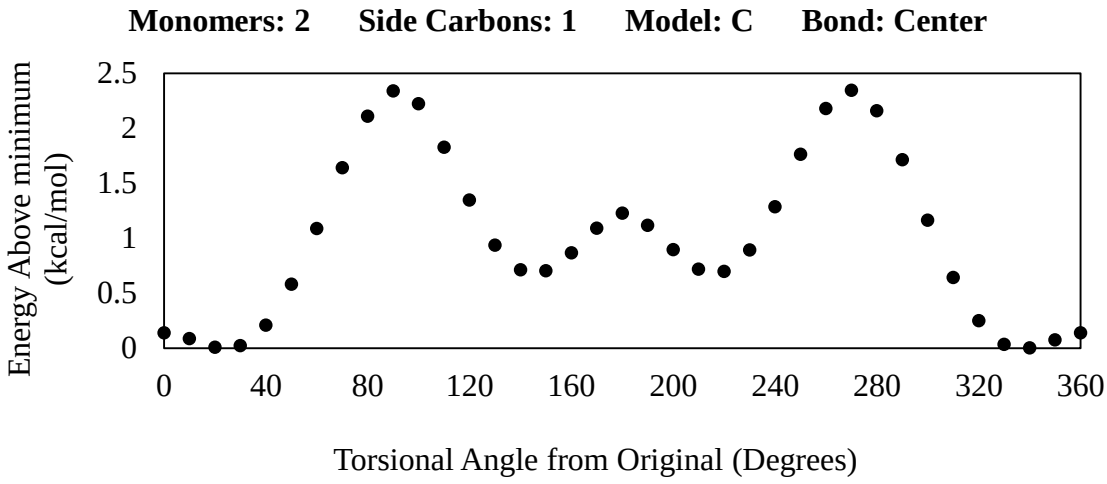
Monomers: 2 Side Carbons: 1 Model: C Bond: Center
Energy Above minimum (kcal/mol)
2.5
2
1.5
1
0.5
0
0 40 80 120 160 200 240 280 320 360
Torsional Angle from Original (Degrees)

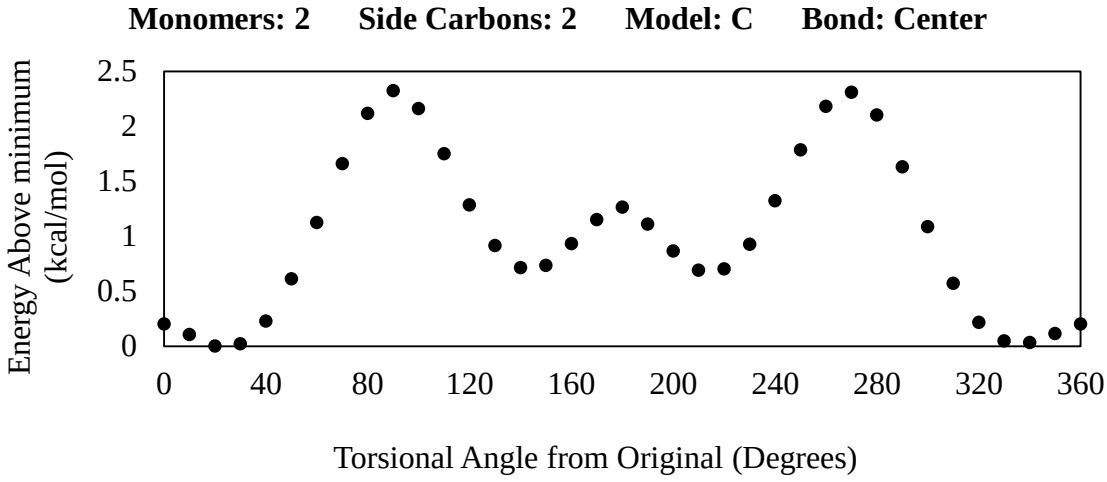
Monomers: 2 Side Carbons: 2 Model: C Bond: Center
Energy Above minimum (kcal/mol)
2.5
2
1.5
1
0.5
0
0 40 80 120 160 200 240 280 320 360
Torsional Angle from Original (Degrees)

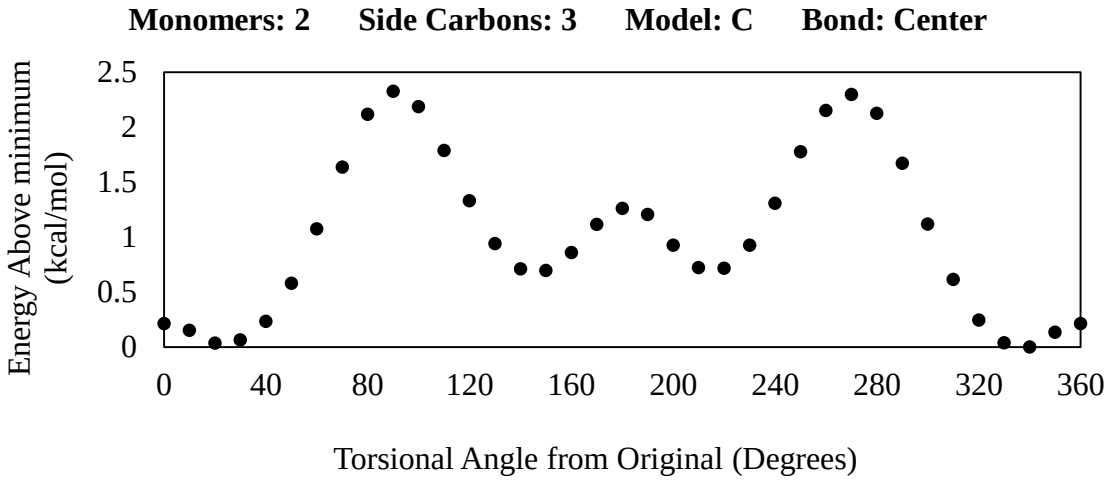
Monomers: 2 Side Carbons: 3 Model: C Bond: Center
Energy Above minimum (kcal/mol)
2.5
2
1.5
1
0.5
0
0 40 80 120 160 200 240 280 320 360
Torsional Angle from Original (Degrees)

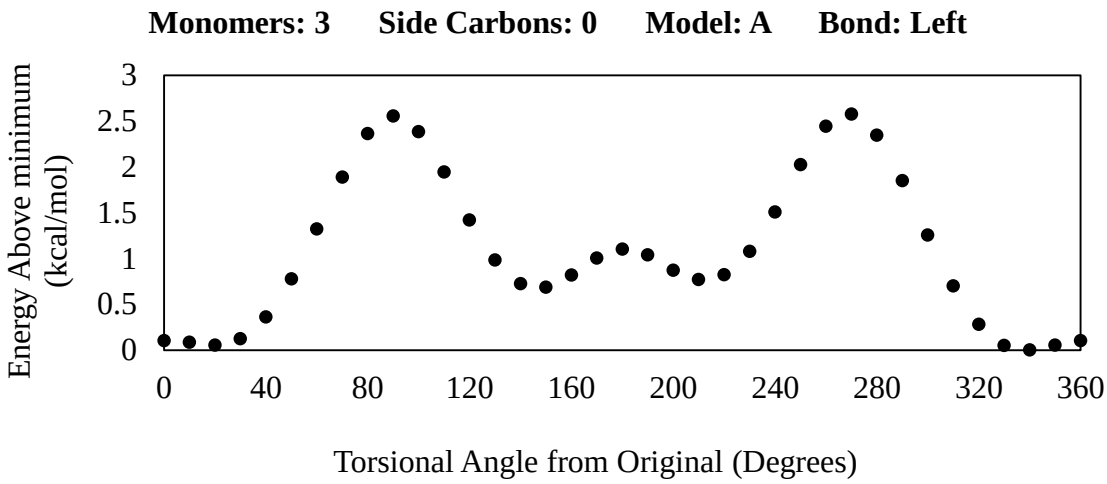
Monomers: 3 Side Carbons: 0 Model: A Bond: Left
Energy Above minimum (kcal/mol)
3
2.5
2
1.5
1
0.5
0
0 40 80 120 160 200 240 280 320 360
Torsional Angle from Original (Degrees)

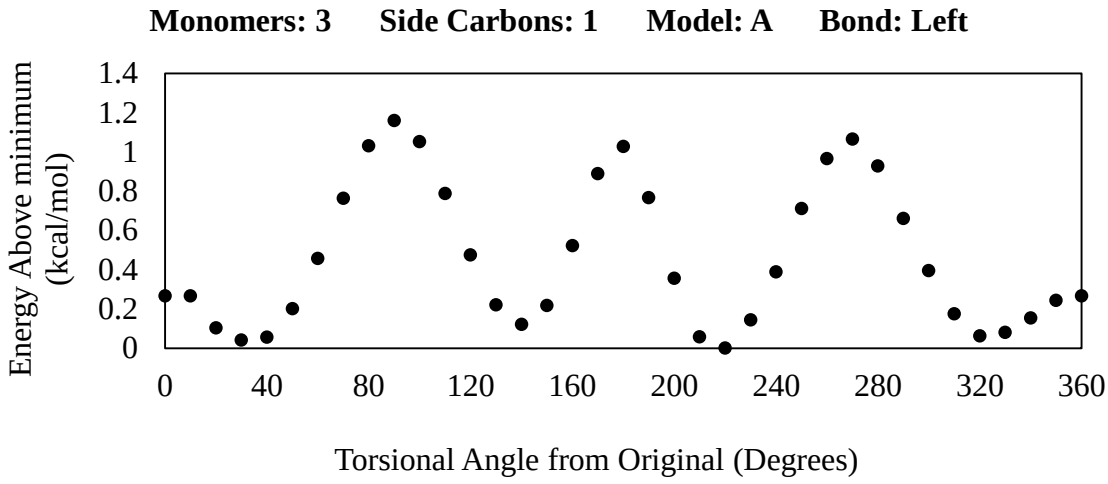
Monomers: 3 Side Carbons: 1 Model: A Bond: Left
Energy Above minimum (kcal/mol)
1.4
1.2
1
0.8
0.6
0.4
0.2
0
0 40 80 120 160 200 240 280 320 360
Torsional Angle from Original (Degrees)

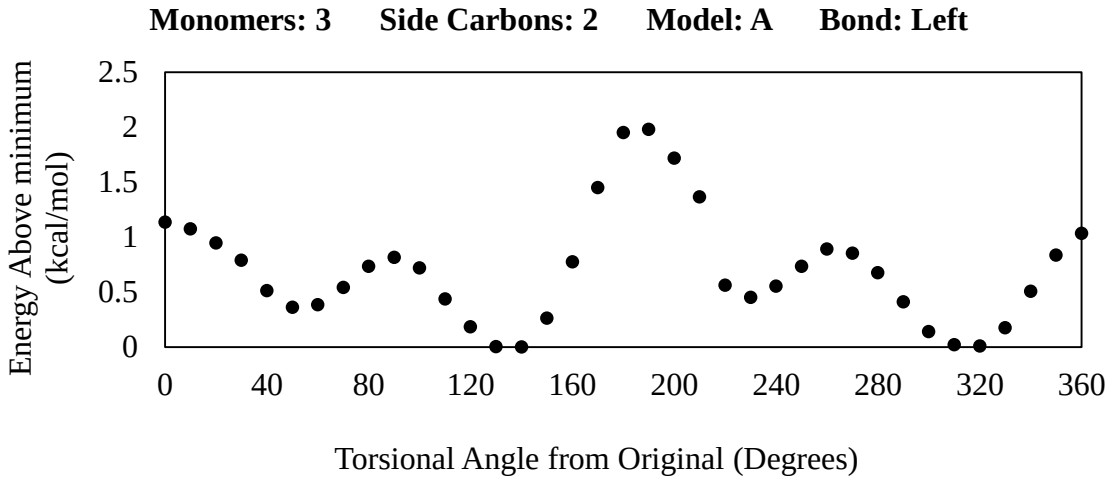
Monomers: 3 Side Carbons: 2 Model: A Bond: Left
Energy Above minimum (kcal/mol)
2.5
2
1.5
1
0.5
0
0 40 80 120 160 200 240 280 320 360
Torsional Angle from Original (Degrees)

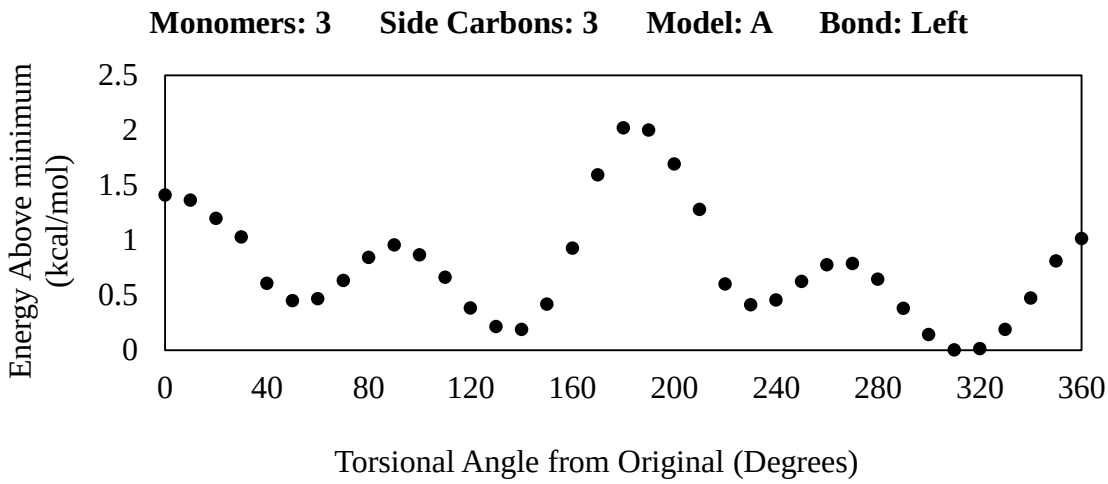
Monomers: 3 Side Carbons: 3 Model: A Bond: Left
Energy Above minimum (kcal/mol)
2.5
2
1.5
1
0.5
0
0 40 80 120 160 200 240 280 320 360
Torsional Angle from Original (Degrees)

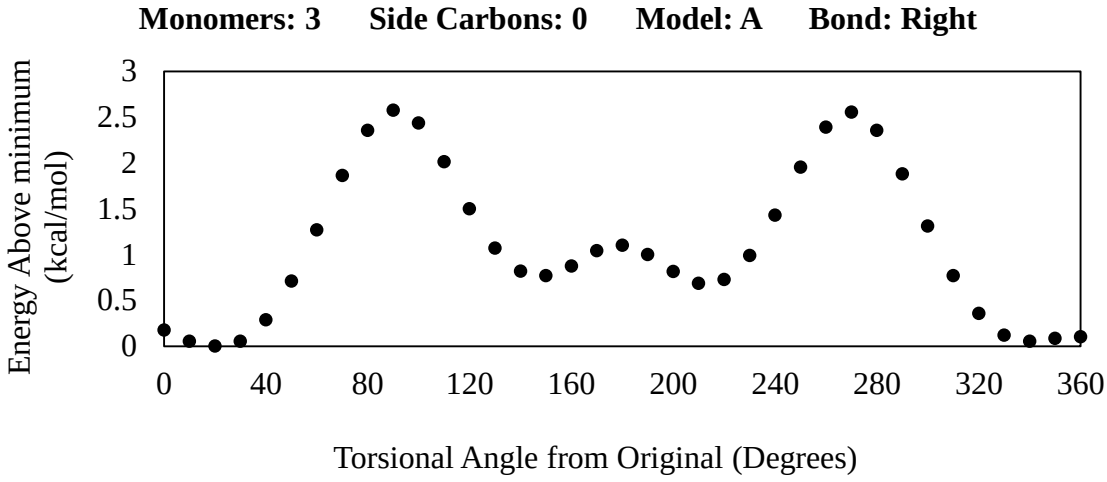
Monomers: 3 Side Carbons: 0 Model: A Bond: Right
Energy Above minimum (kcal/mol)
3
2.5
2
1.5
1
0.5
0
0 40 80 120 160 200 240 280 320 360
Torsional Angle from Original (Degrees)

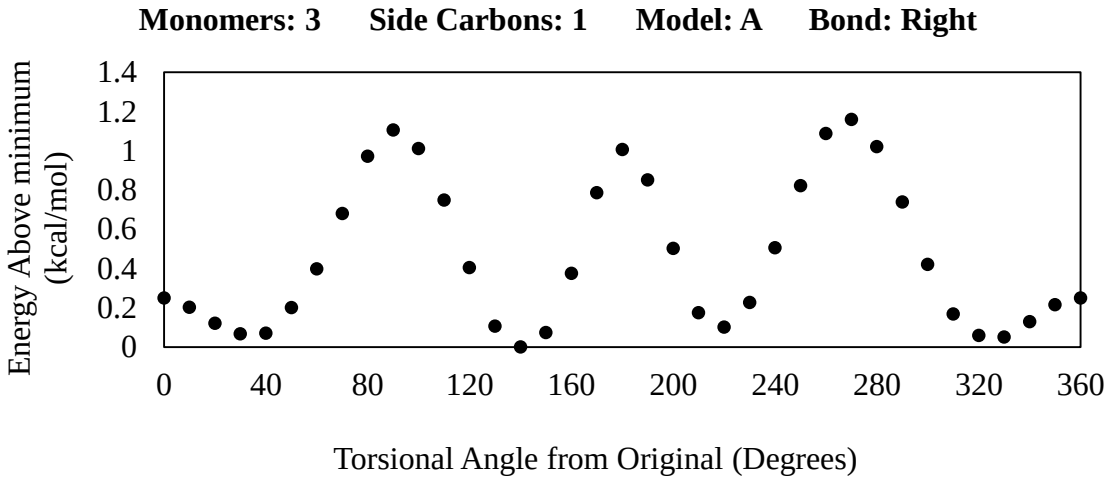
Monomers: 3 Side Carbons: 1 Model: A Bond: Right
Energy Above minimum (kcal/mol)
1.4
1.2
1
0.8
0.6
0.4
0.2
0
0 40 80 120 160 200 240 280 320 360
Torsional Angle from Original (Degrees)

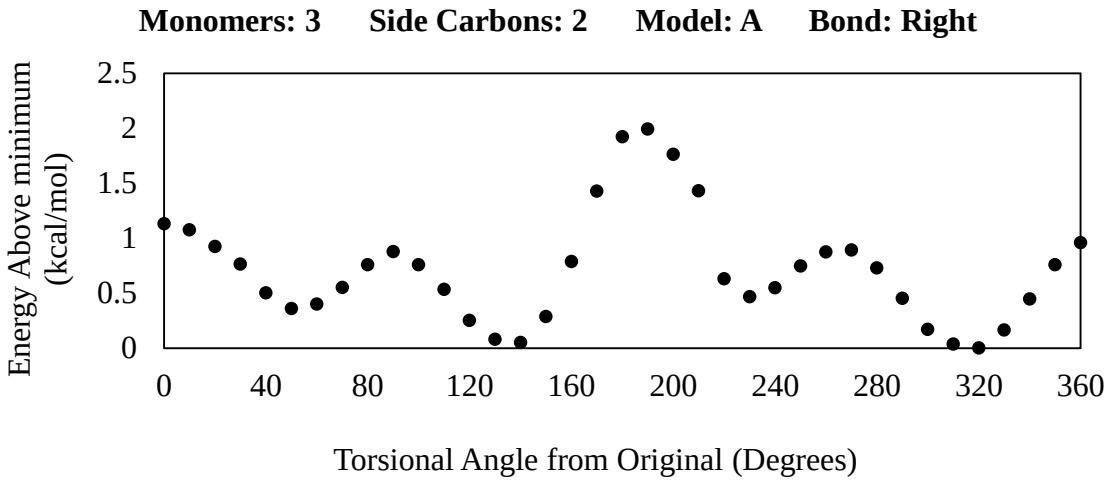
Monomers: 3 Side Carbons: 2 Model: A Bond: Right
Energy Above minimum (kcal/mol)
2.5
2
1.5
1
0.5
0
0 40 80 120 160 200 240 280 320 360
Torsional Angle from Original (Degrees)

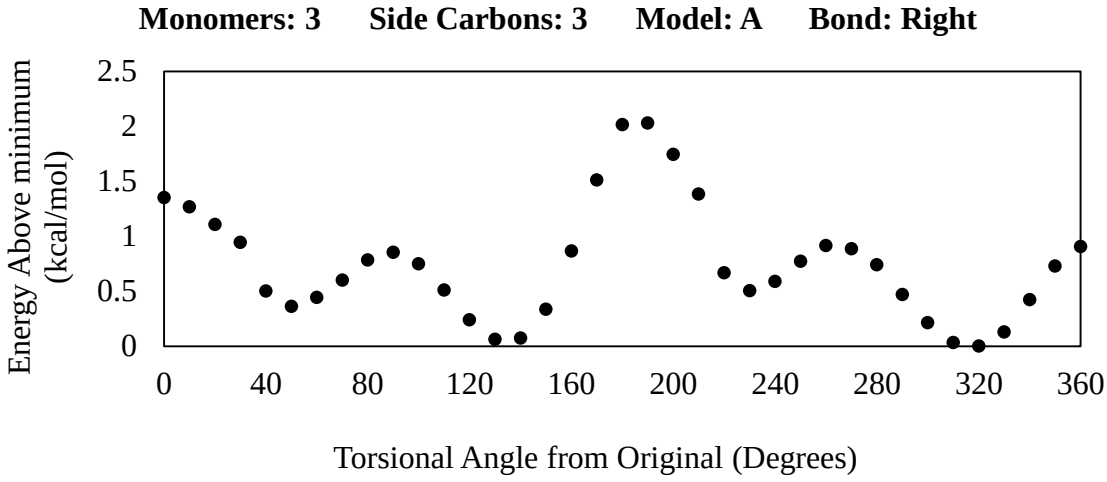
Monomers: 3 Side Carbons: 3 Model: A Bond: Right
Energy Above minimum (kcal/mol)
2.5
2
1.5
1
0.5
0
0 40 80 120 160 200 240 280 320 360
Torsional Angle from Original (Degrees)

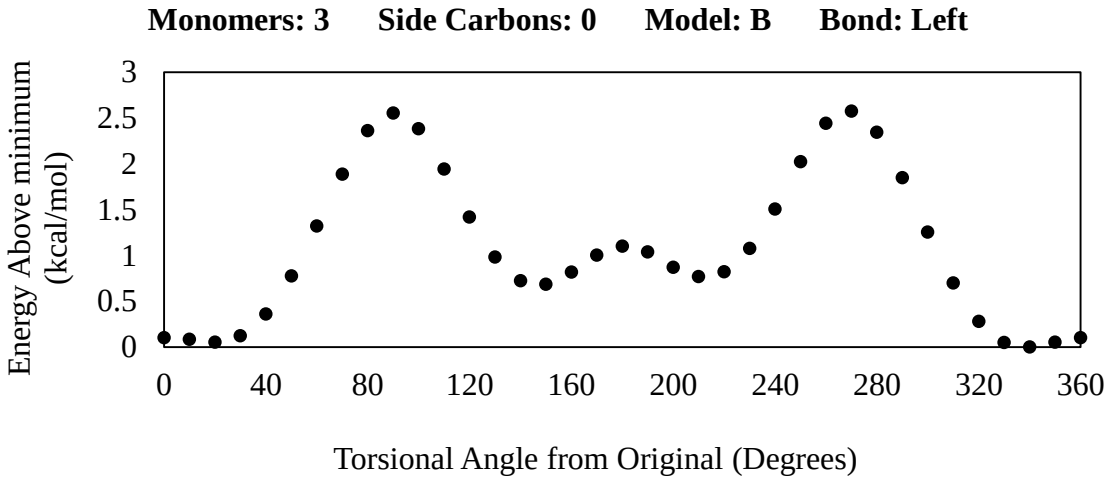
Monomers: 3 Side Carbons: 0 Model: B Bond: Left
Energy Above minimum (kcal/mol)
3
2.5
2
1.5
1
0.5
0
0 40 80 120 160 200 240 280 320 360
Torsional Angle from Original (Degrees)

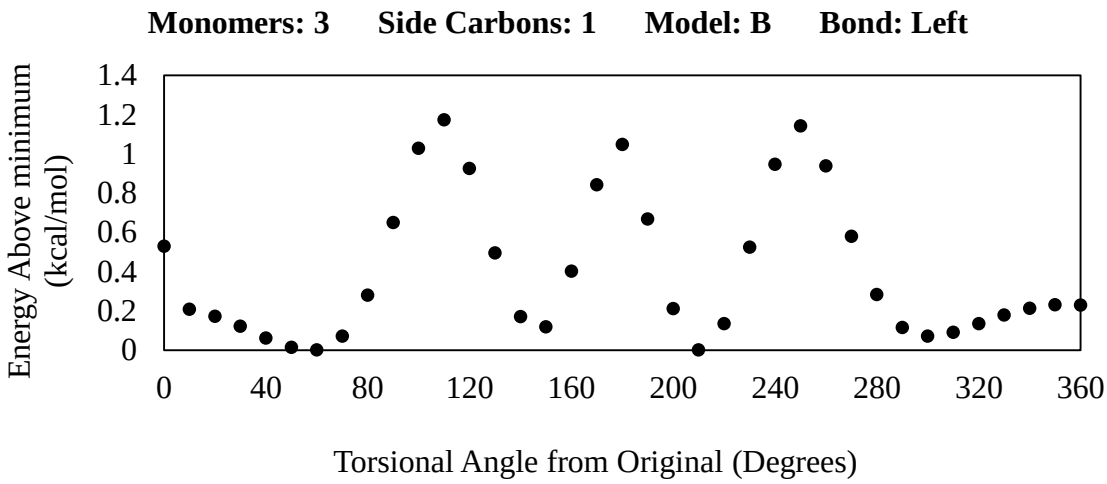
Monomers: 3 Side Carbons: 1 Model: B Bond: Left
Energy Above minimum (kcal/mol)
1.4
1.2
1
0.8
0.6
0.4
0.2
0
0 40 80 120 160 200 240 280 320 360
Torsional Angle from Original (Degrees)

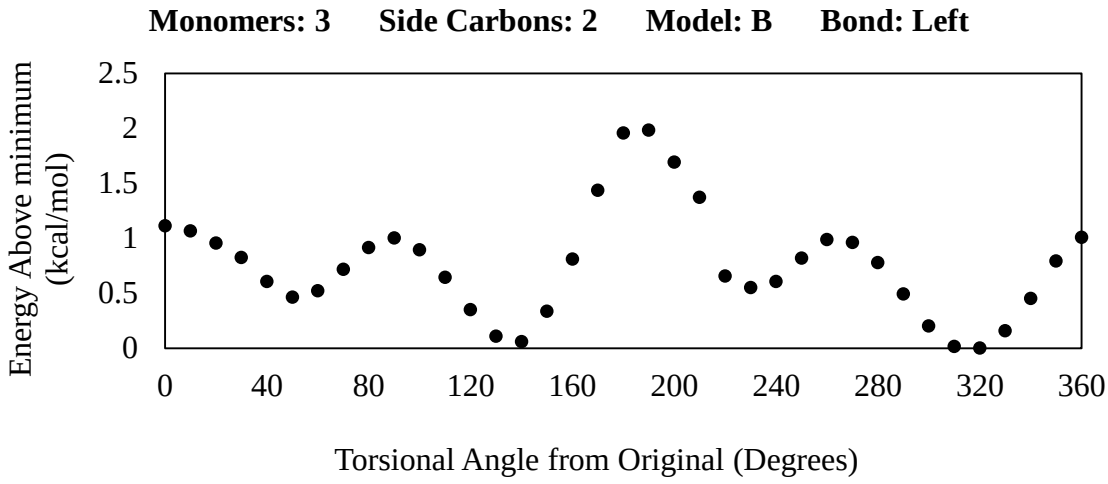
Monomers: 3 Side Carbons: 2 Model: B Bond: Left
Energy Above minimum (kcal/mol)
2.5
2
1.5
1
0.5
0
0 40 80 120 160 200 240 280 320 360
Torsional Angle from Original (Degrees)

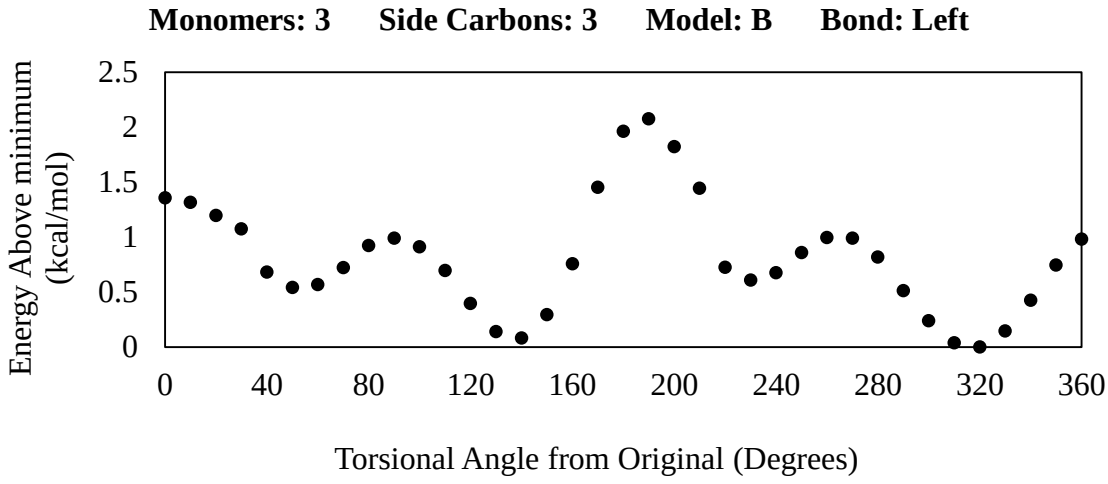
Monomers: 3 Side Carbons: 3 Model: B Bond: Left
Energy Above minimum (kcal/mol)
2.5
2
1.5
1
0.5
0
0 40 80 120 160 200 240 280 320 360
Torsional Angle from Original (Degrees)

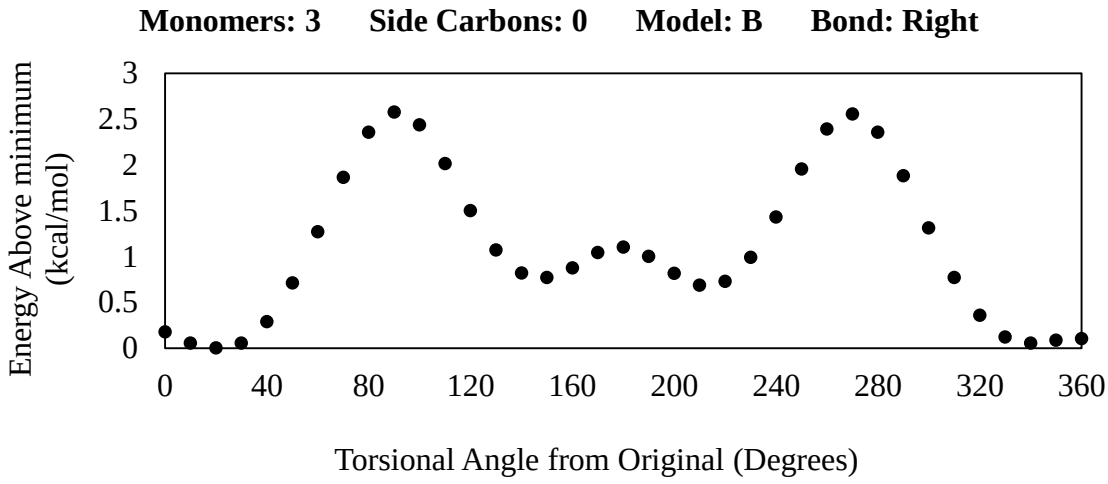
Monomers: 3 Side Carbons: 0 Model: B Bond: Right
Energy Above minimum (kcal/mol)
3
2.5
2
1.5
1
0.5
0
0 40 80 120 160 200 240 280 320 360
Torsional Angle from Original (Degrees)

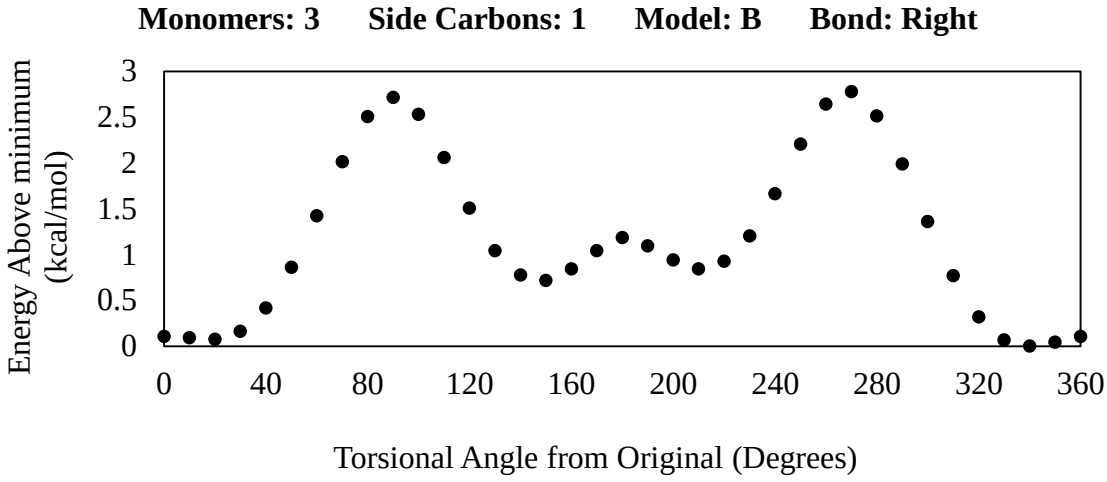
Monomers: 3 Side Carbons: 1 Model: B Bond: Right
Energy Above minimum (kcal/mol)
0
0.5
1
1.5
2
2.5
3
0
40
80
120
160
200
240
280
320
360
Torsional Angle from Original (Degrees)

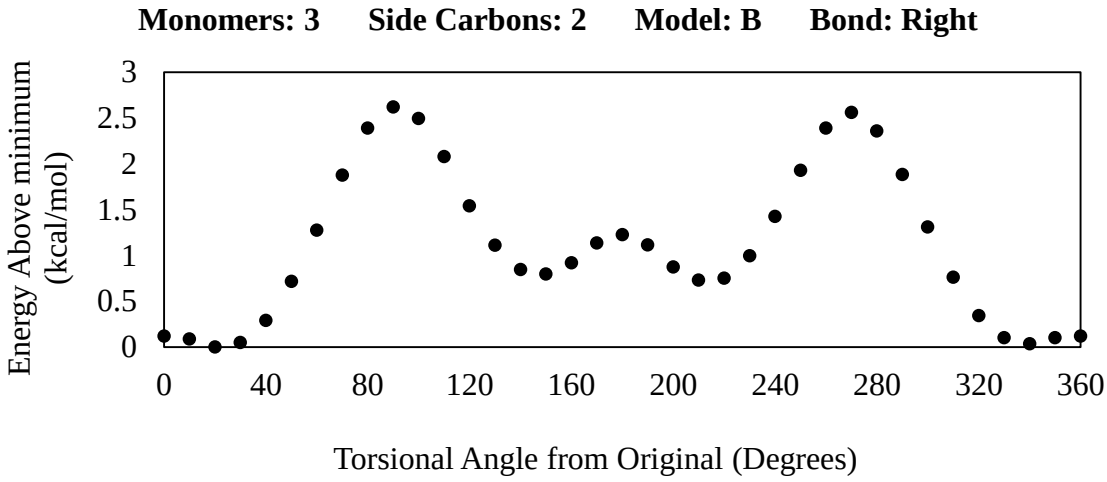
Monomers: 3 Side Carbons: 2 Model: B Bond: Right
Energy Above minimum (kcal/mol)
0
0.5
1
1.5
2
2.5
3
0
40
80
120
160
200
240
280
320
360
Torsional Angle from Original (Degrees)

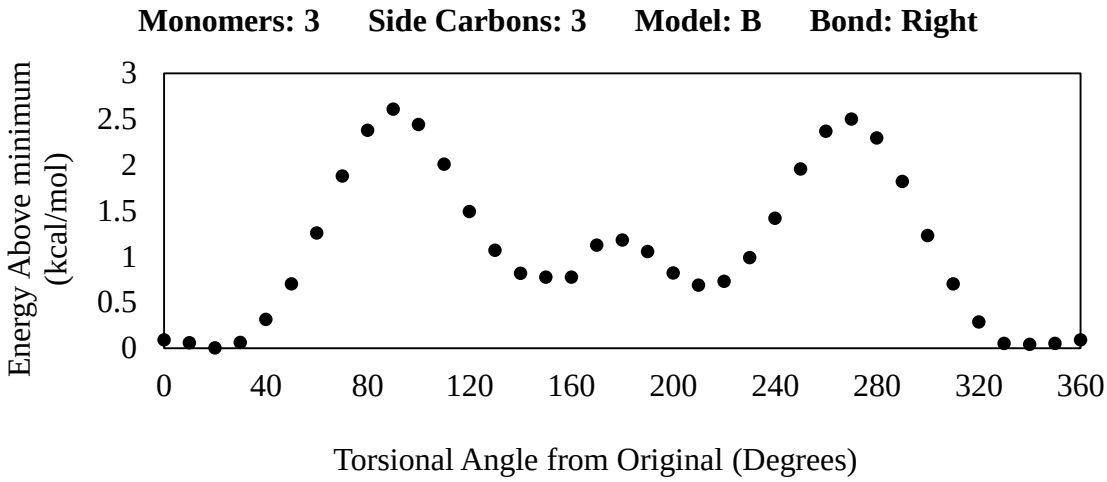
Monomers: 3 Side Carbons: 3 Model: B Bond: Right
Energy Above minimum (kcal/mol)
0
0.5
1
1.5
2
2.5
3
0
40
80
120
160
200
240
280
320
360
Torsional Angle from Original (Degrees)

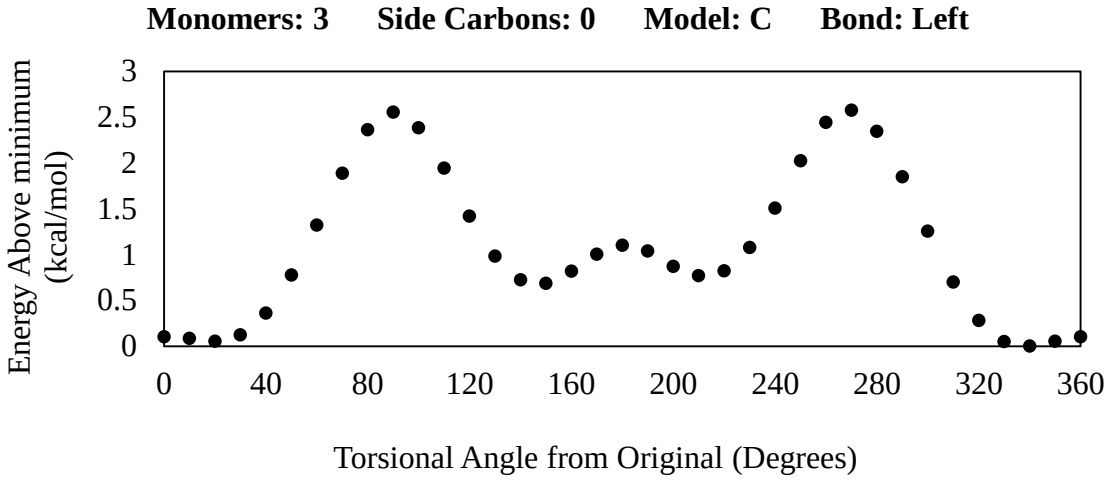
Monomers: 3 Side Carbons: 0 Model: C Bond: Left
Energy Above minimum (kcal/mol)
0
0.5
1
1.5
2
2.5
3
0
40
80
120
160
200
240
280
320
360
Torsional Angle from Original (Degrees)

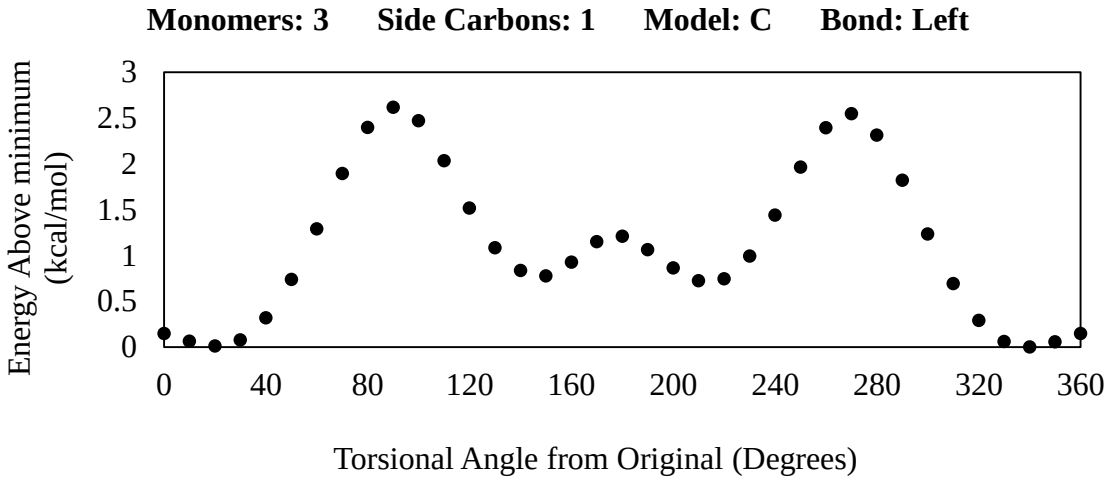
Monomers: 3 Side Carbons: 1 Model: C Bond: Left
Energy Above minimum (kcal/mol)
0
0.5
1
1.5
2
2.5
3
0
40
80
120
160
200
240
280
320
360
Torsional Angle from Original (Degrees)

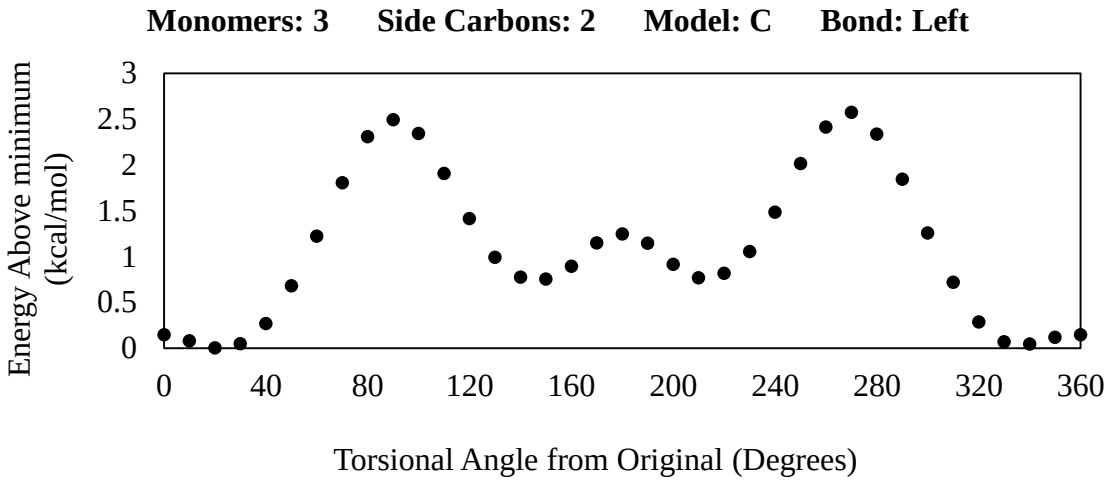
Monomers: 3 Side Carbons: 2 Model: C Bond: Left
Energy Above minimum (kcal/mol)
0
0.5
1
1.5
2
2.5
3
0
40
80
120
160
200
240
280
320
360
Torsional Angle from Original (Degrees)

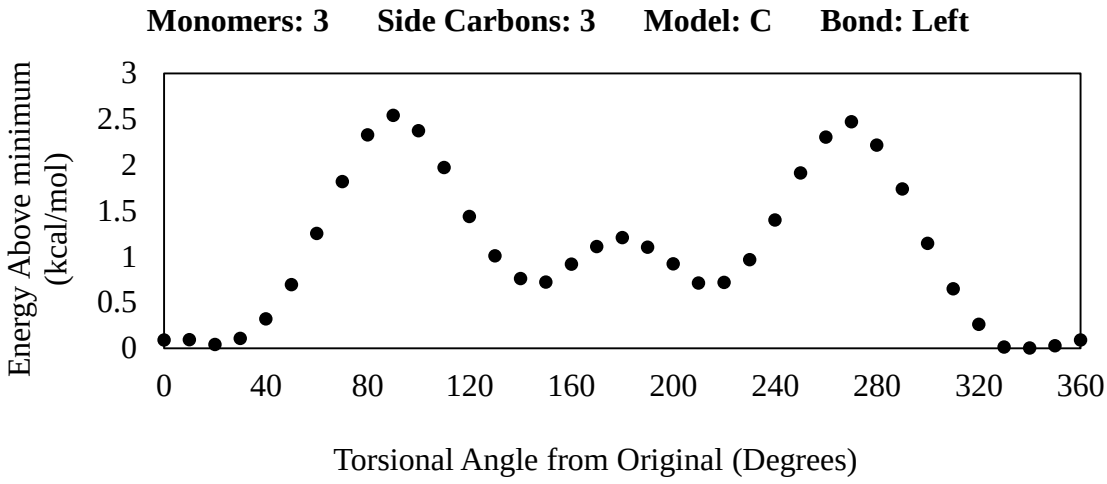
Monomers: 3 Side Carbons: 3 Model: C Bond: Left
Energy Above minimum (kcal/mol)
3
2.5
2
1.5
1
0.5
0
0 40 80 120 160 200 240 280 320 360
Torsional Angle from Original (Degrees)

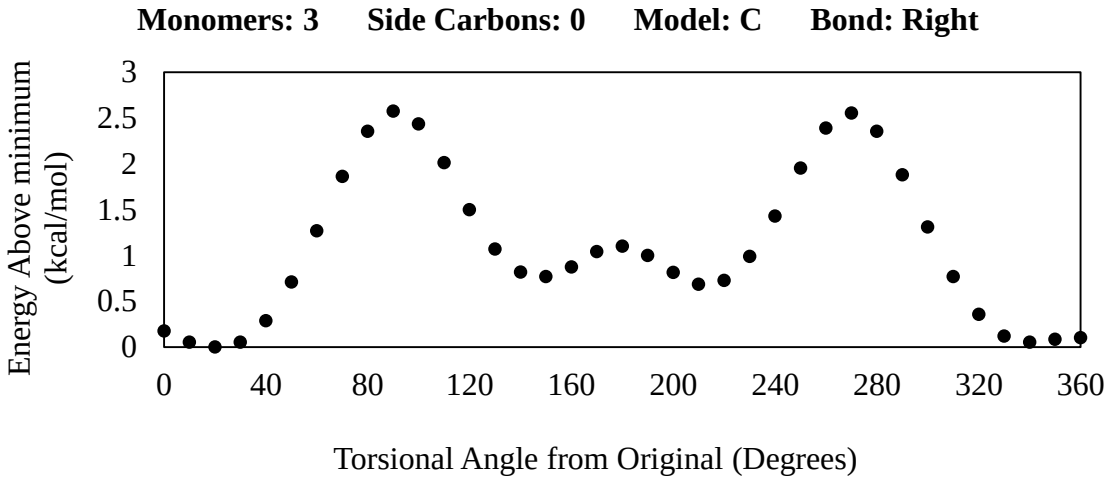
Monomers: 3 Side Carbons: 0 Model: C Bond: Right
Energy Above minimum (kcal/mol)
3
2.5
2
1.5
1
0.5
0
0 40 80 120 160 200 240 280 320 360
Torsional Angle from Original (Degrees)

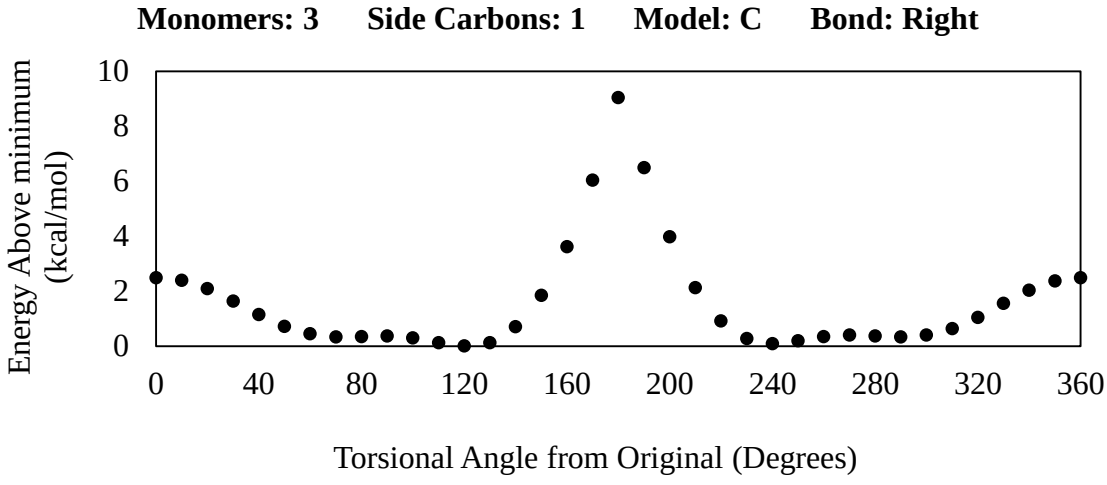
Monomers: 3 Side Carbons: 1 Model: C Bond: Right
Energy Above minimum (kcal/mol)
10
8
6
4
2
0
0 40 80 120 160 200 240 280 320 360
Torsional Angle from Original (Degrees)

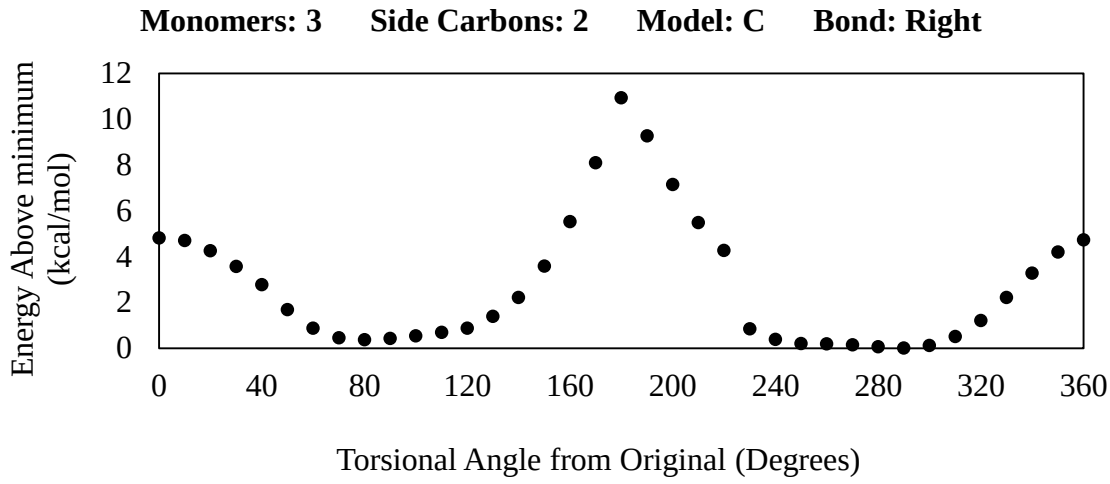
Monomers: 3 Side Carbons: 2 Model: C Bond: Right
Energy Above minimum (kcal/mol)
0
2
4
6
8
10
12
0
40
80
120
160
200
240
280
320
360
Torsional Angle from Original (Degrees)

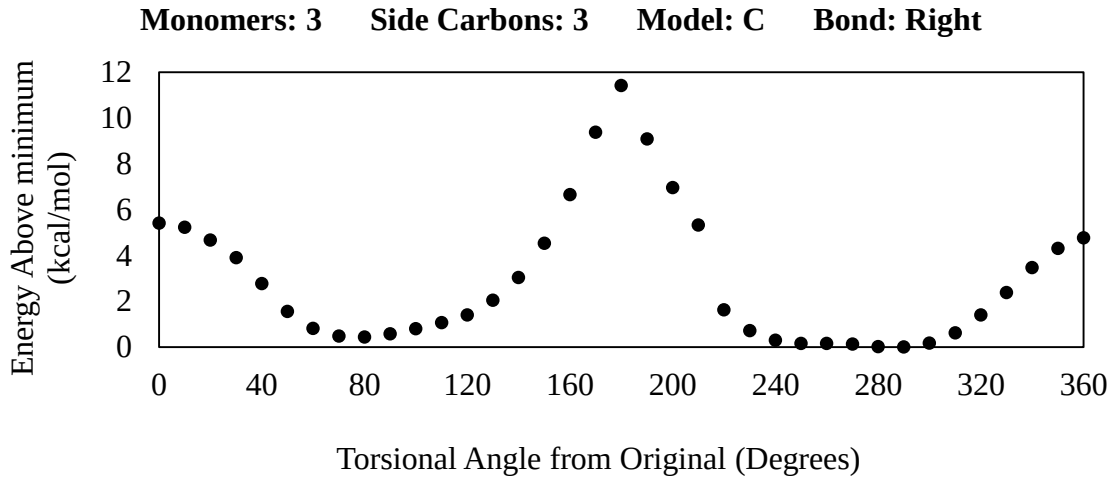
Monomers: 3 Side Carbons: 3 Model: C Bond: Right
Energy Above minimum (kcal/mol)
0
2
4
6
8
10
12
0
40
80
120
160
200
240
280
320
360
Torsional Angle from Original (Degrees)

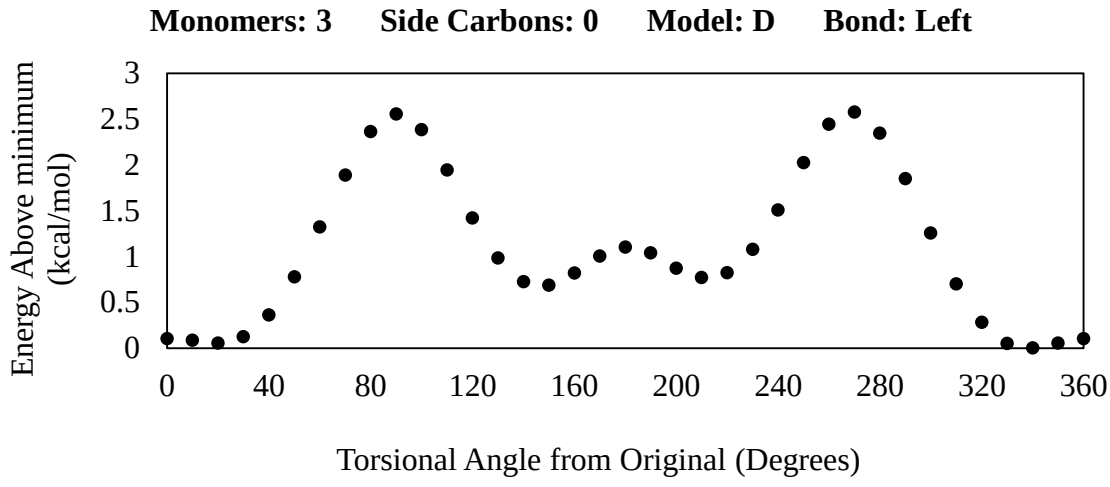
Monomers: 3 Side Carbons: 0 Model: D Bond: Left
Energy Above minimum (kcal/mol)
0
0.5
1
1.5
2
2.5
3
0
40
80
120
160
200
240
280
320
360
Torsional Angle from Original (Degrees)

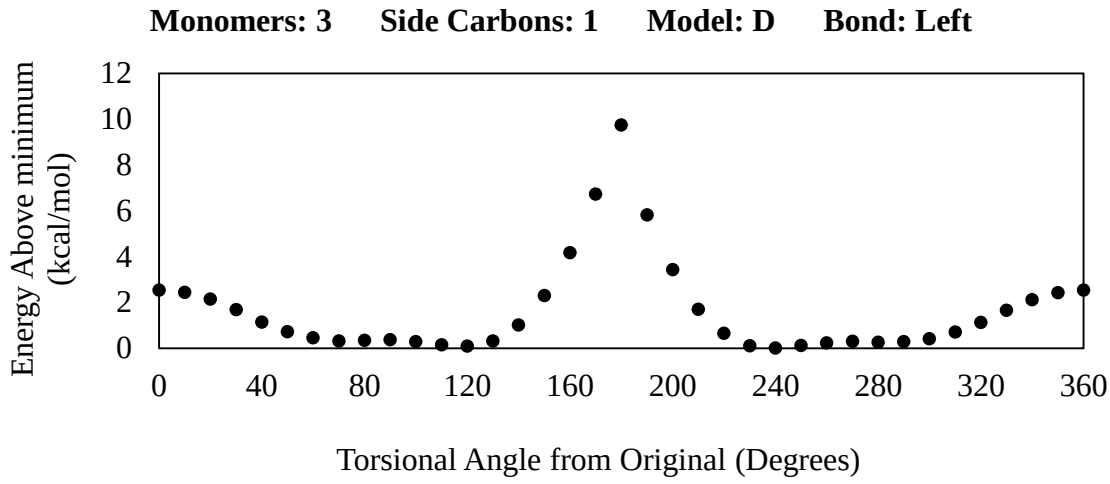
Monomers: 3 Side Carbons: 1 Model: D Bond: Left
Energy Above minimum (kcal/mol)
0
2
4
6
8
10
12
0
40
80
120
160
200
240
280
320
360
Torsional Angle from Original (Degrees)

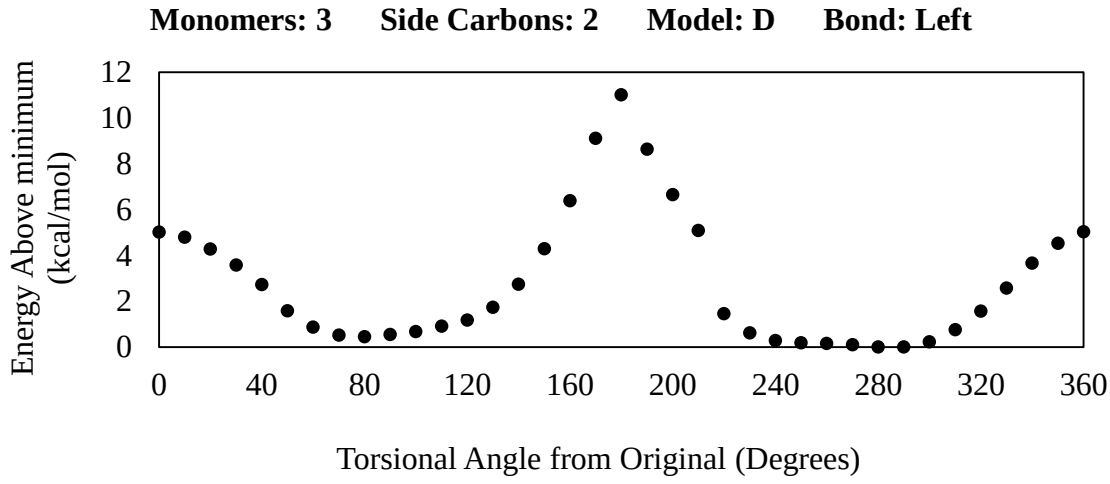
Monomers: 3 Side Carbons: 2 Model: D Bond: Left
Energy Above minimum (kcal/mol)
0
2
4
6
8
10
12
0
40
80
120
160
200
240
280
320
360
Torsional Angle from Original (Degrees)

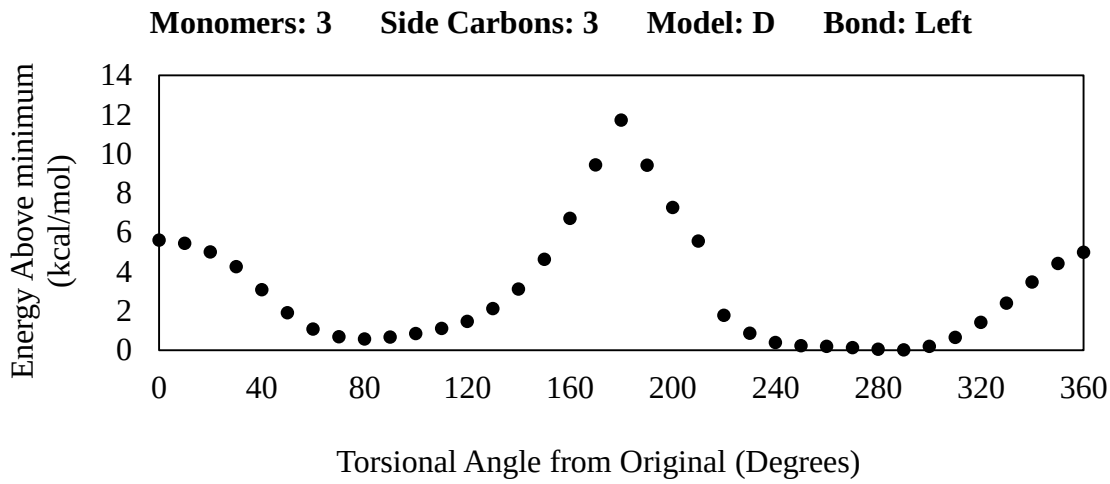
Monomers: 3 Side Carbons: 3 Model: D Bond: Left
Energy Above minimum (kcal/mol)
0
2
4
6
8
10
12
14
0
40
80
120
160
200
240
280
320
360
Torsional Angle from Original (Degrees)

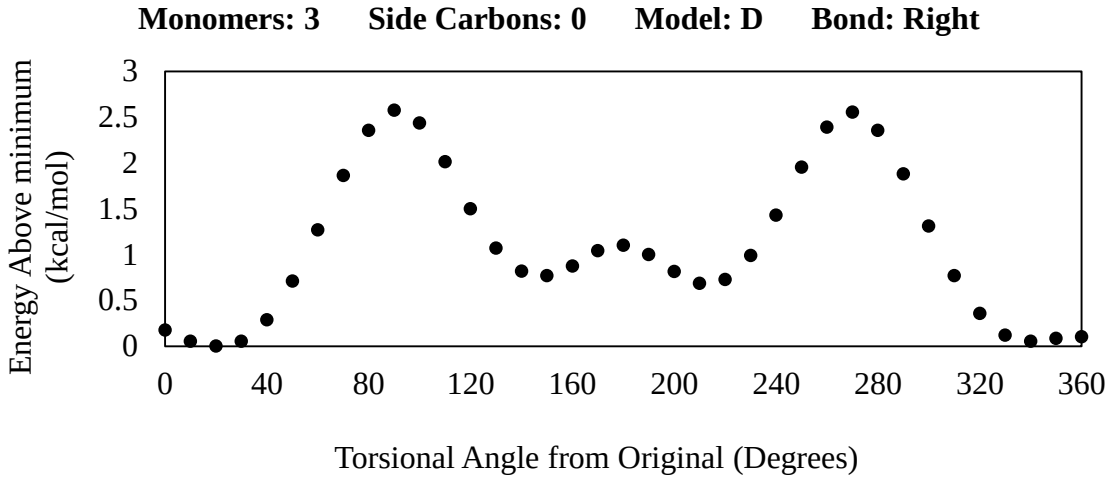
Monomers: 3 Side Carbons: 0 Model: D Bond: Right
Energy Above minimum (kcal/mol)
0
0.5
1
1.5
2
2.5
3
0
40
80
120
160
200
240
280
320
360
Torsional Angle from Original (Degrees)

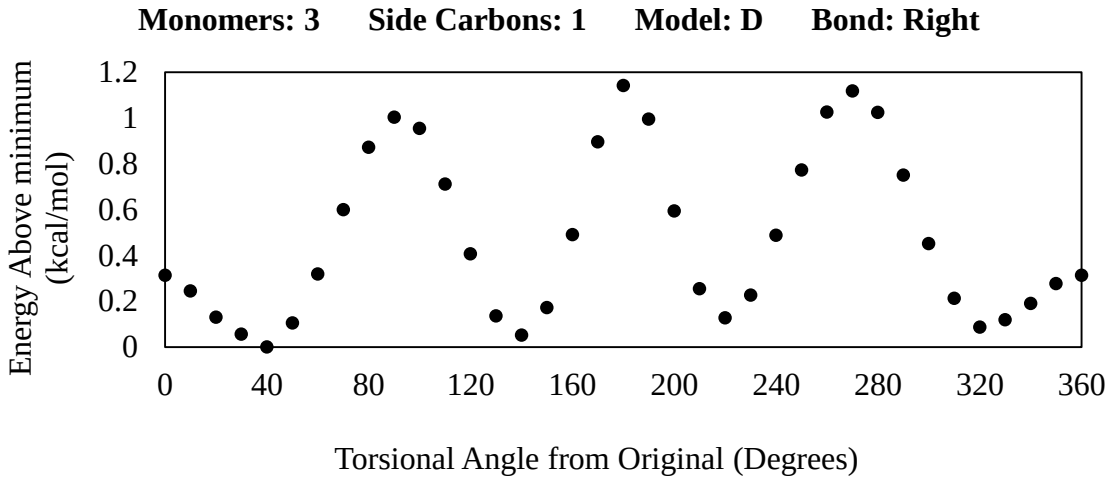
Monomers: 3 Side Carbons: 1 Model: D Bond: Right
Energy Above minimum (kcal/mol)
0
0.2
0.4
0.6
0.8
1
1.2
0
40
80
120
160
200
240
280
320
360
Torsional Angle from Original (Degrees)

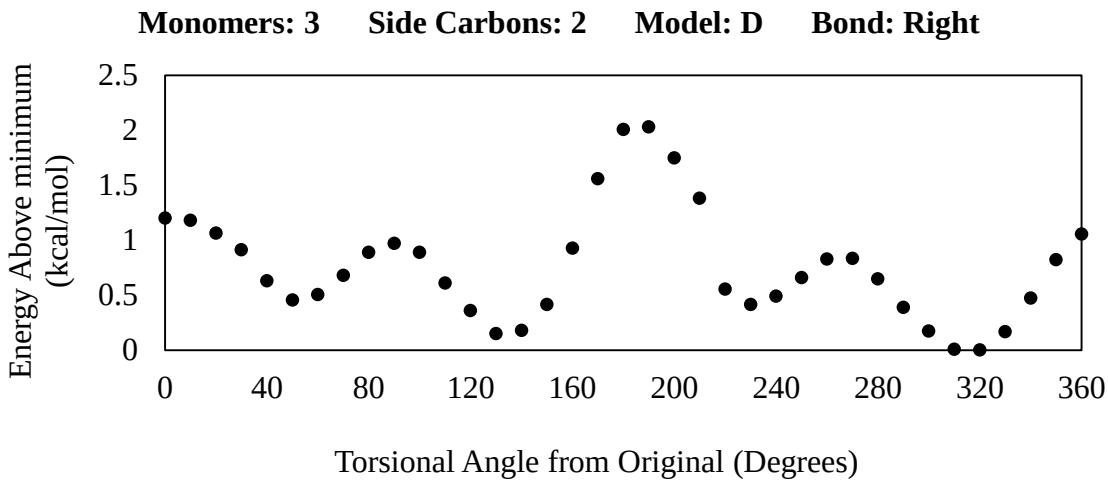
Monomers: 3 Side Carbons: 2 Model: D Bond: Right
Energy Above minimum (kcal/mol)
0
0.5
1
1.5
2
2.5
0
40
80
120
160
200
240
280
320
360
Torsional Angle from Original (Degrees)

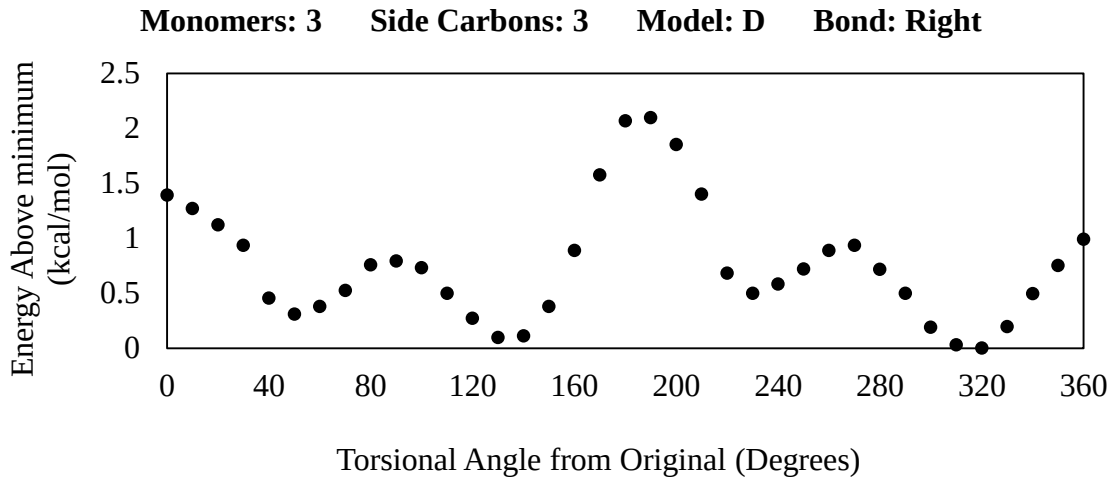
Monomers: 3 Side Carbons: 3 Model: D Bond: Right
Energy Above minimum (kcal/mol)
2.5
2
1.5
1
0.5
0
0
40
80
120
160
200
240
280
320
360
Torsional Angle from Original (Degrees)

Appendix B

Selection of Relevant Torsional Profiles: PBTTT

This appendix is the collection of energy as a function of torsional angle compiled for all possible arrangements PBTTT, which includes the placement of equivalently-sized hydrogen, methyl, ethyl, and propyl functional groups which would be considered simplified models of regioregular (RR) or regiorandom (RRa) PBTTT. Each of the following graphs is labeled with the number of carbons in the functionalization, the model letter for the number of monomers in the model, and the bond which was constrained in the optimization.

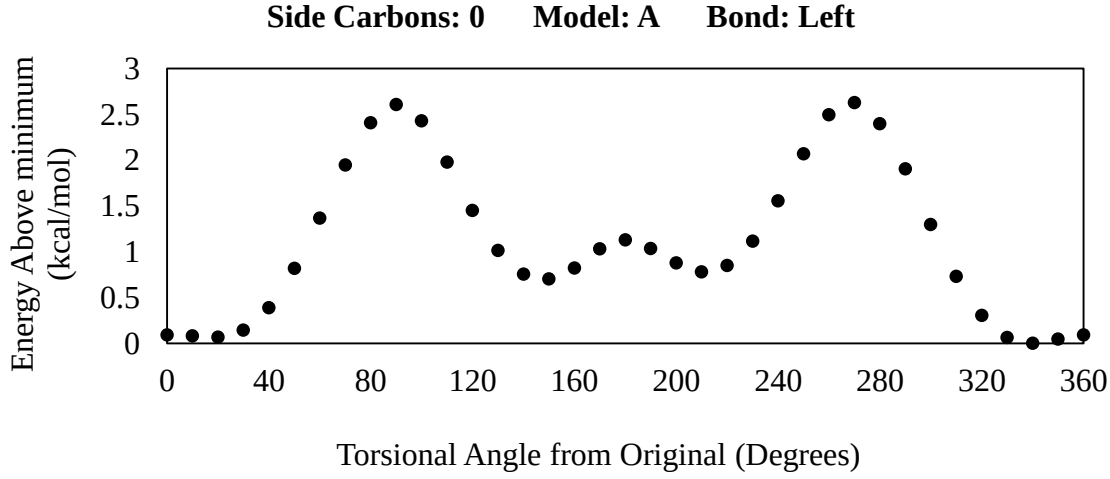

Side Carbons: 1 Model: A Bond: Left

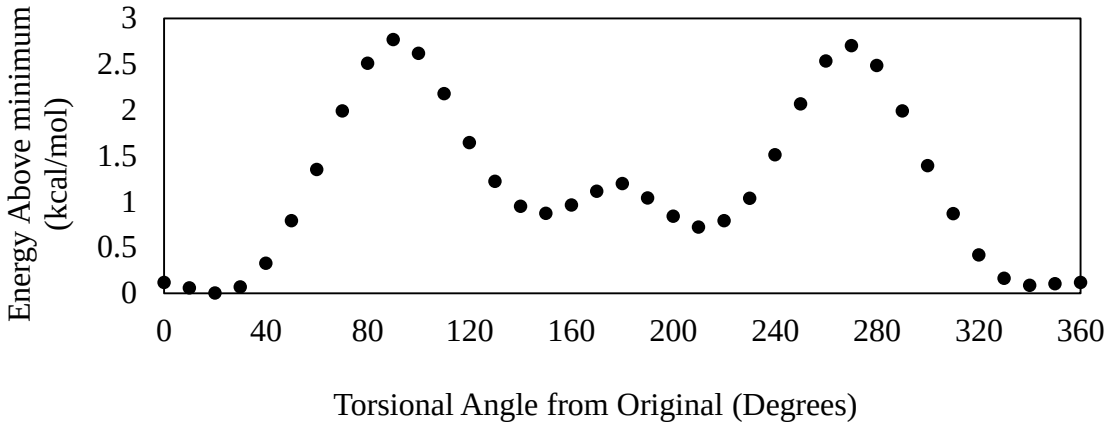

Side Carbons: 2 Model: A Bond: Left

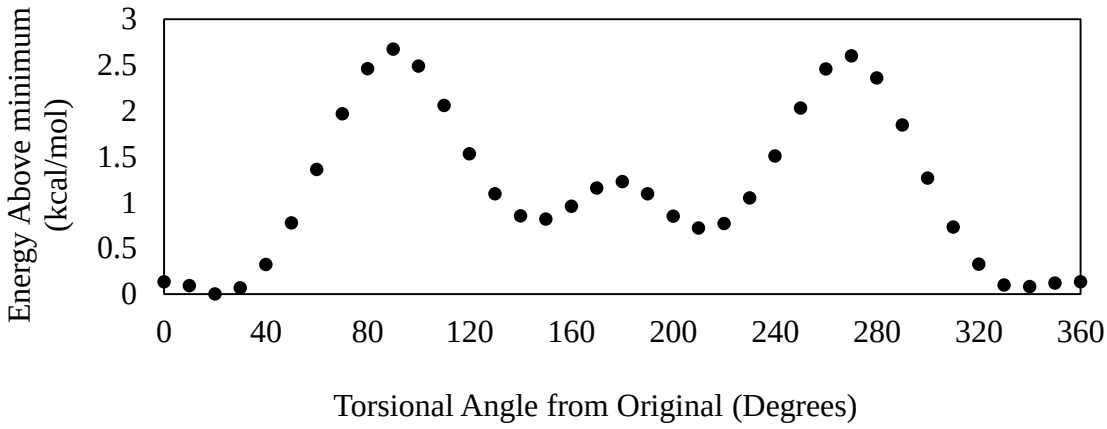

Side Carbons: 3 Model: A Bond: Left

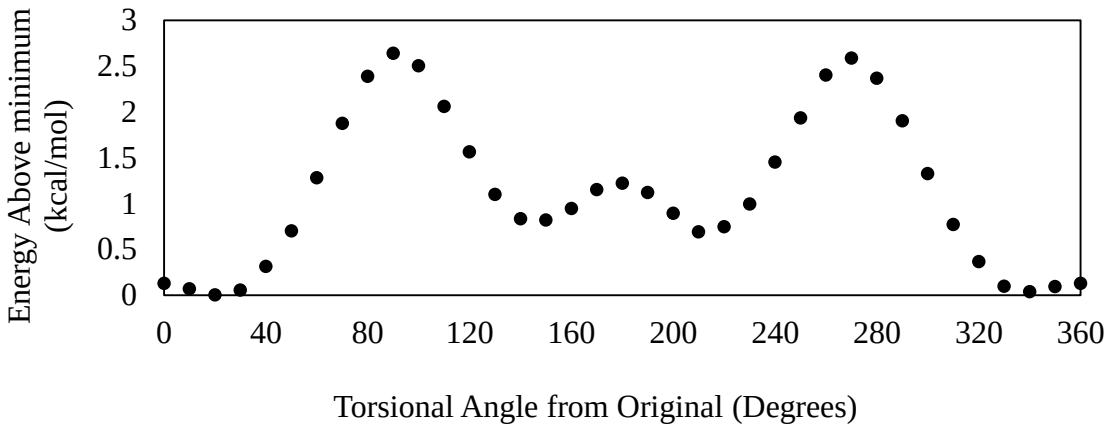

Side Carbons: 0 Model: A Bond: Right

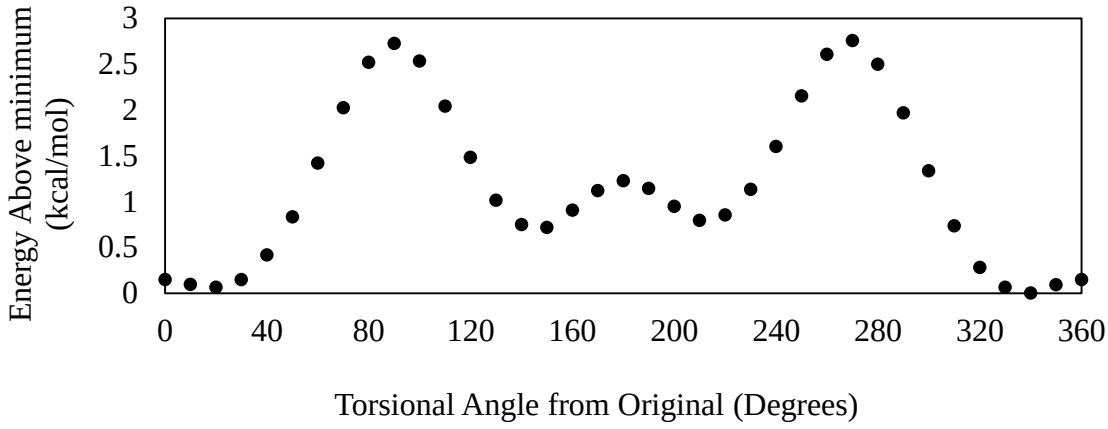

Side Carbons: 1 Model: A Bond: Right

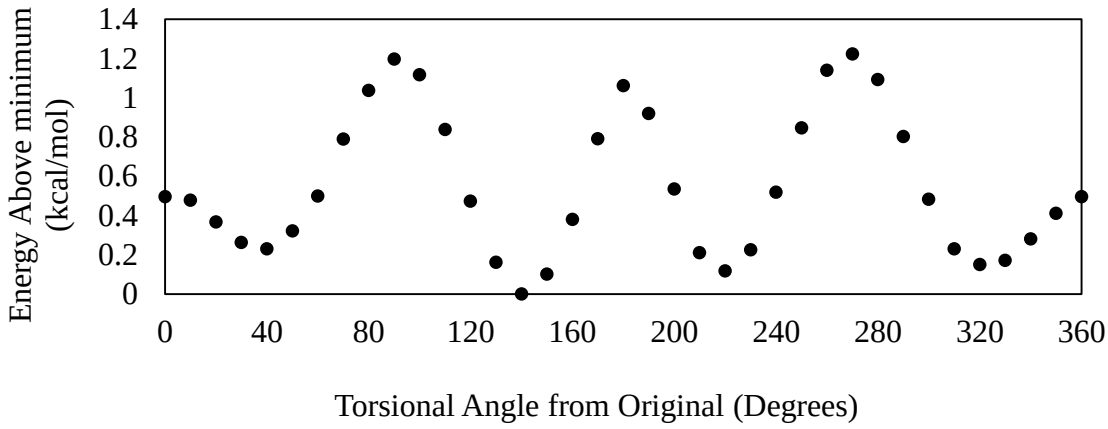

Side Carbons: 2 Model: A Bond: Right

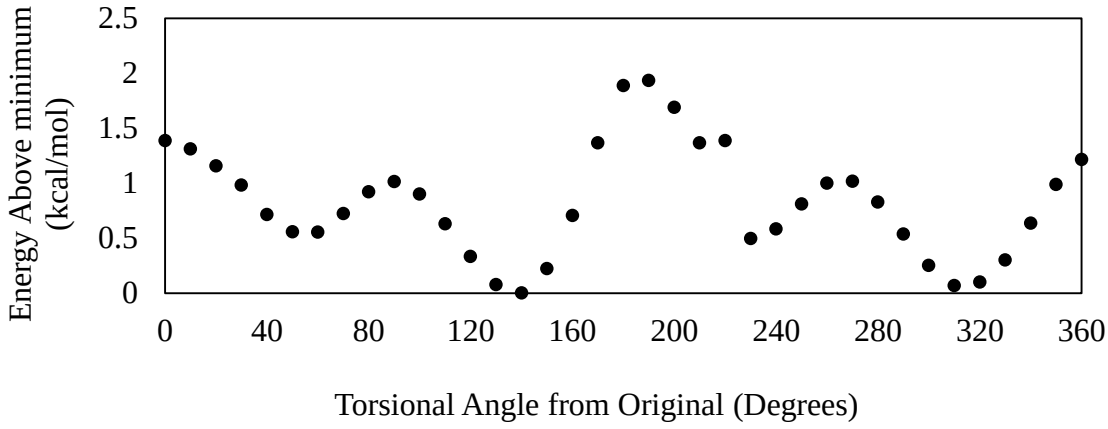

Side Carbons: 3 Model: A Bond: Right

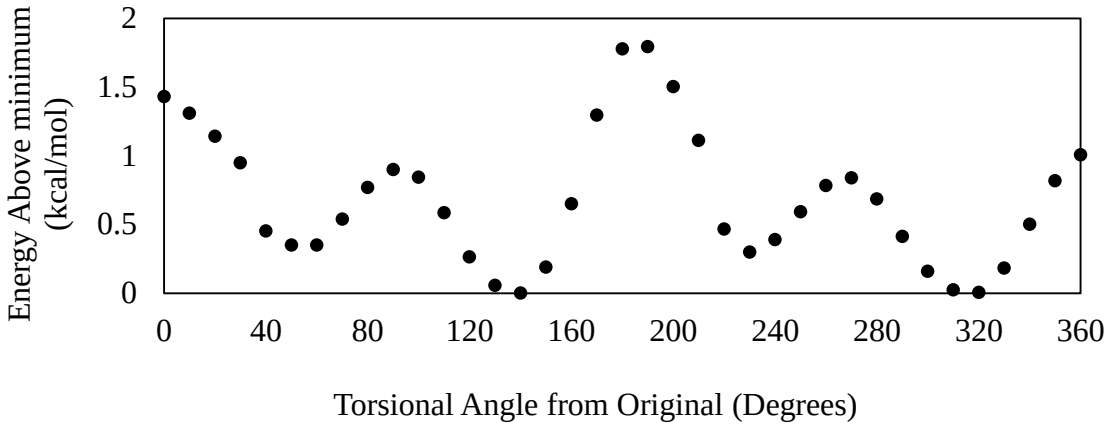

Side Carbons: 0 Model: B Bond: Left

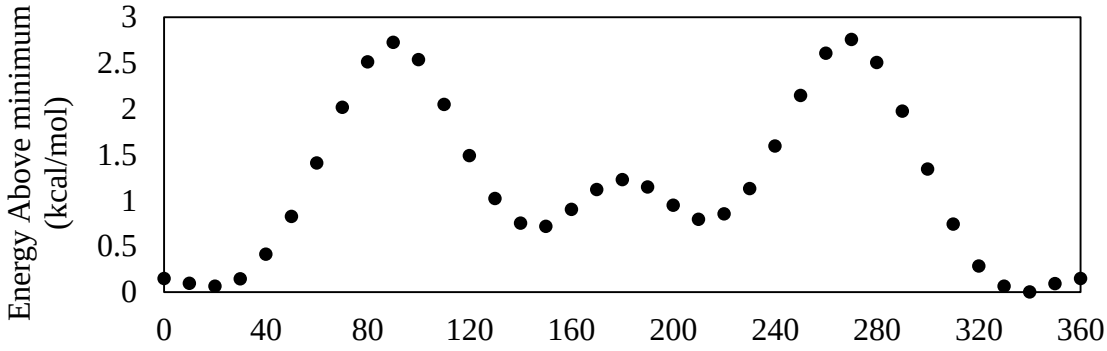

Side Carbons: 1 Model: B Bond: Left

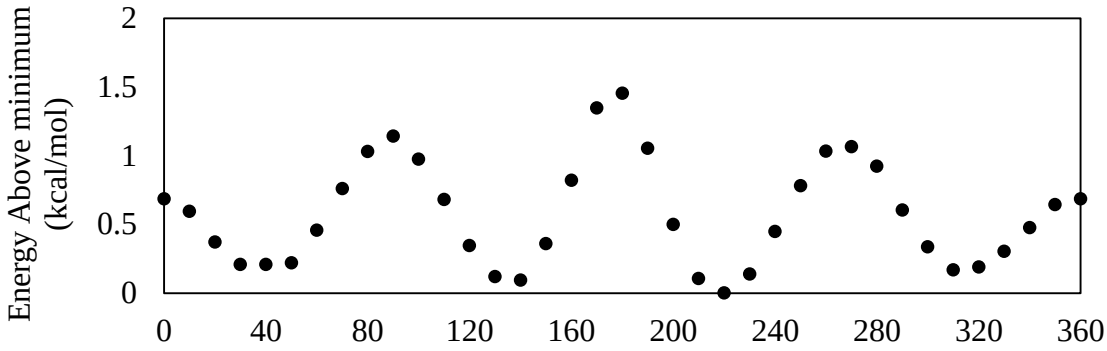

Side Carbons: 2 Model: B Bond: Left

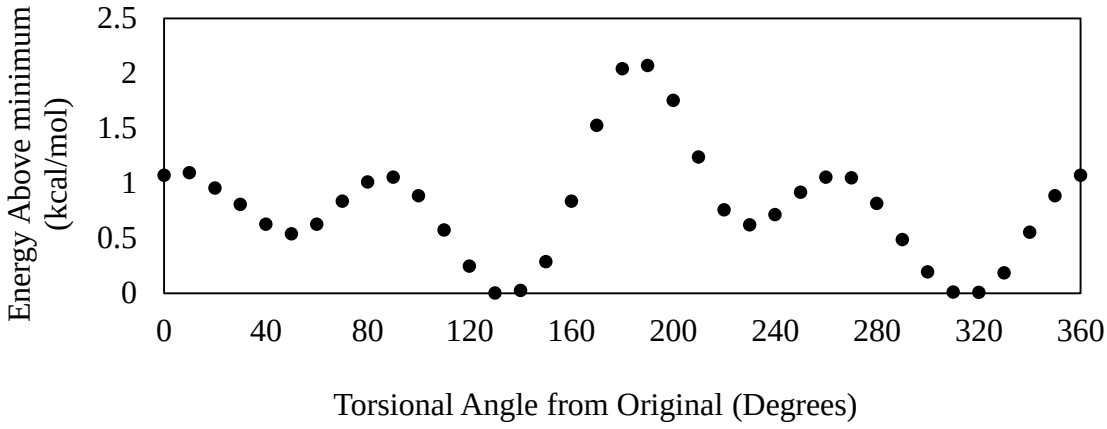

Side Carbons: 3 Model: B Bond: Left

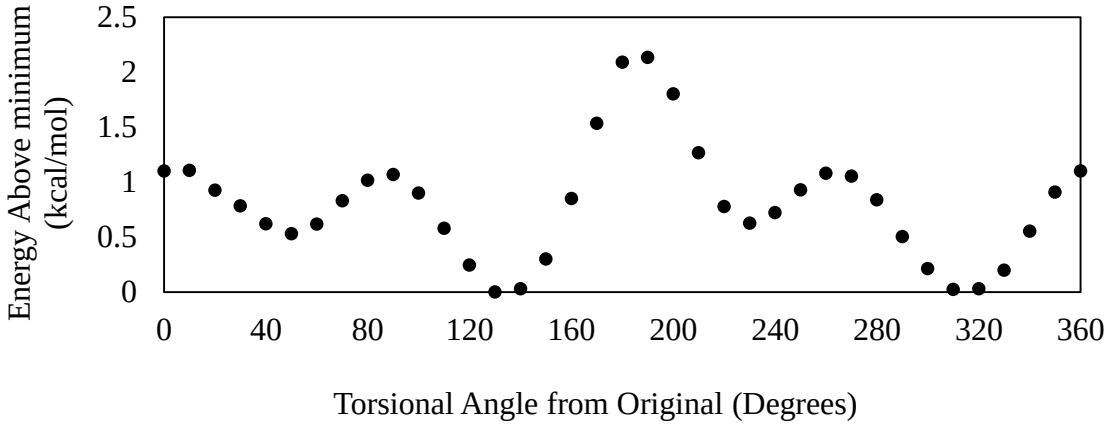

Side Carbons: 0 Model: B Bond: Right

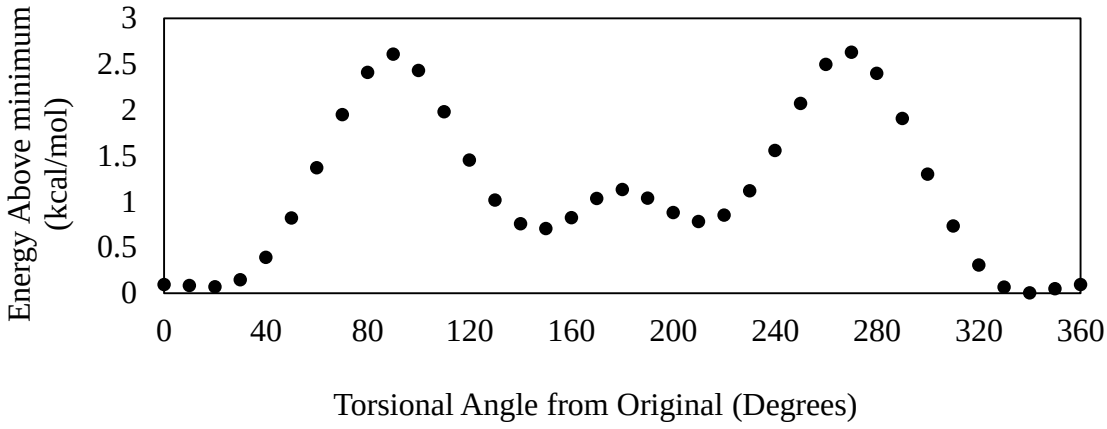

Side Carbons: 1 Model: B Bond: Right

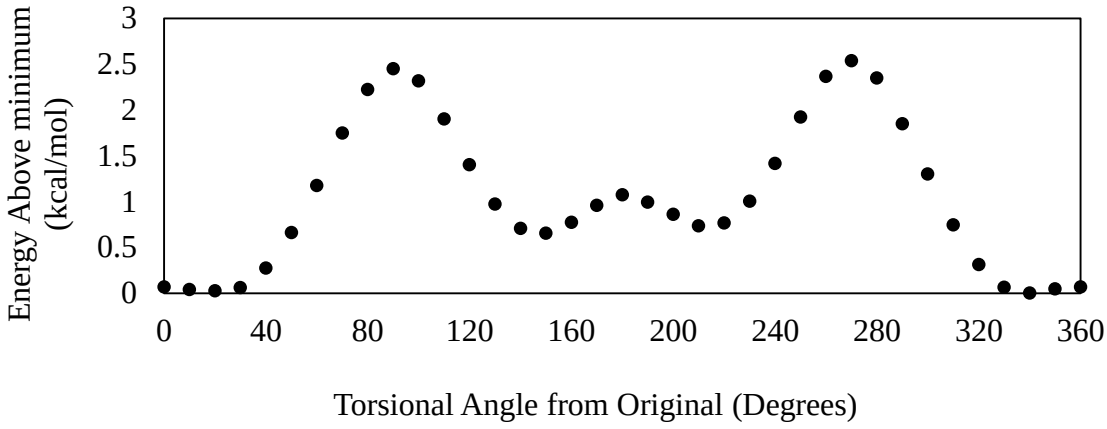

Side Carbons: 2 Model: B Bond: Right

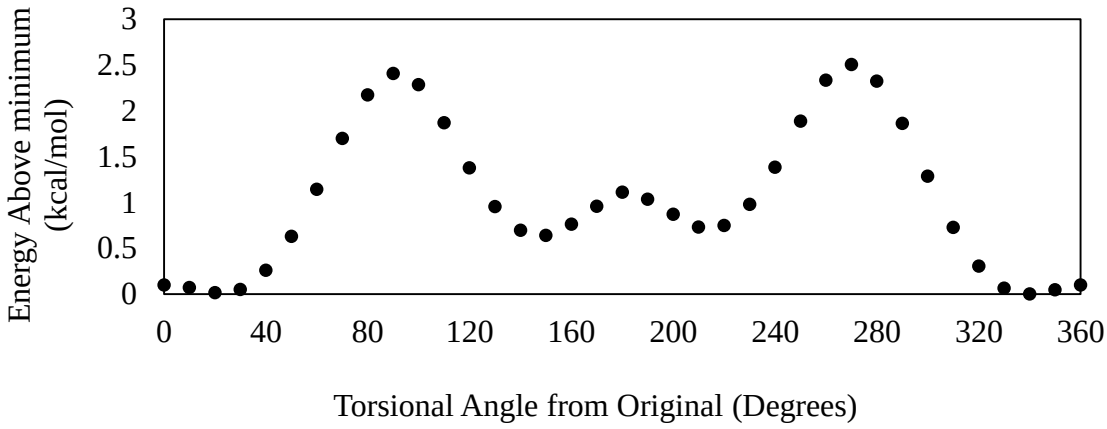

Side Carbons: 3 Model: B Bond: Right

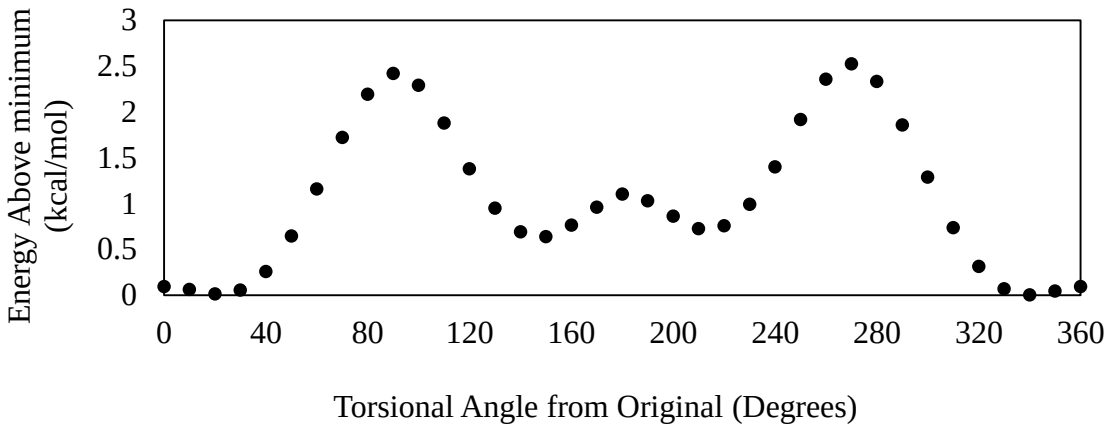

BIBLIOGRAPHY

1) Beljonne, David, et al. "Electronic Processes at Organic− Organic Interfaces: Insight from Modeling and Implications for Opto-electronic Devices†." *Chemistry of Materials* 23.3 (2010): 591-609.

2) Brédas, Jean-Luc, et al. "Molecular understanding of organic solar cells: the challenges." *Accounts of chemical research* 42.11 (2009): 1691-1699.

3) Cave, Robert J., and Marshall D. Newton. "Calculation of electronic coupling matrix elements for ground and excited state electron transfer reactions: comparison of the generalized Mulliken–Hush and block diagonalization methods." *The Journal of chemical physics* 106.22 (1997): 9213-9226.

4) Cave, Robert J., and Marshall D. Newton. "Generalization of the Mulliken-Hush treatment for the calculation of electron transfer matrix elements." *Chemical physics letters* 249.1 (1996): 15-19.

5) Chong, Song-Ho, et al. "Molecular Theory for the Nonequilibrium Free Energy Profile in Electron Transfer Reaction." *The Journal of Physical Chemistry* 99.26 (1995): 10526-10529.

6) van Eijck, Lambert, Mark R. Johnson, and Gordon J. Kearley. "Intermolecular interactions in bithiophene as a model for polythiophene." *The Journal of Physical Chemistry A* 107.42 (2003): 8980-8984.

7) Fang, Xiao-Hong, et al. "Theoretical study on charge transport properties of a dinuclear aluminum 8-hydroxyquinoline complex." *Journal of Molecular Structure: THEOCHEM* 896.1 (2009): 44-48.

8) Grozema, Ferdinand C., et al. "Intramolecular charge transport along isolated chains of conjugated polymers: effect of torsional disorder and polymerization defects." *The Journal of Physical Chemistry B* 106.32 (2002): 7791-7795.

9) Hush, N. S. "Homogeneous and heterogeneous optical and thermal electron transfer." *Electrochimica Acta* 13.5 (1968): 1005-1023.

10) Janssen, René AJ, Jan C. Hummelen, and N. Serdar Sariciftci. "Polymer–fullerene bulk heterojunction solar cells." *MRS bulletin* 30.01 (2005): 33-36.

11) Kwon, O., et al. "Characterization of the molecular parameters determining charge transport in anthradithiophene." *The Journal of chemical physics* 120.17 (2004): 8186-8194.

12) Lemaur, Vincent, et al. "Photoinduced charge generation and recombination dynamics in model donor/acceptor pairs for organic solar cell applications: a full quantum-chemical treatment." *Journal of the American Chemical Society* 127.16 (2005): 6077-6086.

13) Linares, Mathieu, et al. "On the Interface Dipole at the Pentacene− Fullerene Heterojunction: A Theoretical Study." *The Journal of Physical Chemistry C* 114.7 (2010): 3215-3224.

14) Liu, Jianhua, et al. "Insight into how molecular structures of thiophene-based conjugated polymers affect crystallization behaviors." Polymer 52.10 (2011): 2302-2309.

15) Mulliken, Robert S. "Molecular compounds and their spectra. II." *Journal of the American Chemical Society* 74.3 (1952): 811-824.

16) Northrup, John E. "Atomic and electronic structure of polymer organic semiconductors: P3HT, PQT, and PBTTT." *Physical Review B* 76.24 (2007): 245202.

17) Shaheen, Sean E., David S. Ginley, and Ghassan E. Jabbour. "Organic-based photovoltaics: toward low-cost power generation." *MRS bulletin* 30.01 (2005): 10-19.

18) Thompson, Barry C., and Jean MJ Fréchet. "Polymer–fullerene composite solar cells." *Angewandte Chemie International Edition* 47.1 (2008): 58-77.

19) Vanlaeke, Peter, et al. "P3HT/PCBM bulk heterojunction solar cells: Relation between morphology and electro-optical characteristics." *Solar Energy Materials and Solar Cells* 90.14 (2006): 2150-2158.

20) Yi, Yuanping, Veaceslav Coropceanu, and Jean-Luc Brédas. "Exciton-dissociation and charge-recombination processes in pentacene/C60 solar cells: theoretical insight into the impact of interface geometry." *Journal of the American Chemical Society* 131.43 (2009): 15777-15783.

ACADEMIC VITA

Grant Elledge

121 W. Fairmount Ave., Apt. F-1, State College, PA 16801

717-449-8754

Education

B.S. Chemical Engineering, The Pennsylvania State University	May 2014
Honors in Chemical Engineering, Schreyer Honors College	May 2014

Honors and Awards

Myriant Corporation Scholarship for Excellence in Energy Research	May 2013
Student Leader Scholarship *3-time Recipient*	2011-2013
Best Design Communication Award, Industry-Sponsored Design	April 2011
President's Freshman Award	Feb. 2011

Association Memberships/Activities

Executive Leader and Group Leader, Alliance Christian Fellowship *President* *Vice President*	2011-2014 *2013-2014* *2012-2013*
Member, Springfield Benefitting the Penn State Dance Marathon (THON)	2010-2014

Professional Experience

Marketing Intern, Air Products and Chemicals, Inc.	Sum. 2013
Research and Development Intern, 3M Company	Sum. 2012
Undergraduate Researcher, Department of Chemical Engineering	Sum. 2011

Professional Presentations

Research Experience for Undergraduates Final Presentation	July 2011
Penn State Speech CAS 100A Speech Competition *Competition Finalist*	Nov. 2010